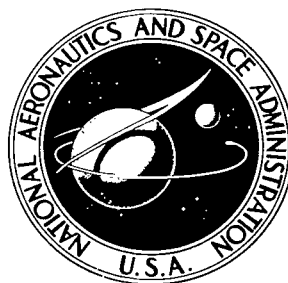


**NASA TECHNICAL NOTE**



**NASA TN D-6402**

C.1

**NASA TN D-6402**

**LOAN COPY: RETURN  
AFWL (DOGL)  
KIRTLAND AFB, N.**



**SUBCOOLED- AND NET-BOILING  
HEAT TRANSFER TO LOW-PRESSURE  
WATER IN ELECTRICALLY HEATED TUBES**

*by James R. Stone*

*Lewis Research Center  
Cleveland, Ohio 44135*



0132913

1. Report No. NASA TN D-6402		2. Government Accession No.		3. Recipient's Catalog No.	
4. Title and Subtitle SUBCOOLED- AND NET-BOILING HEAT TRANSFER TO LOW-PRESSURE WATER IN ELECTRICALLY HEATED TUBES				5. Report Date July 1971	
7. Author(s) James R. Stone				6. Performing Organization Code	
9. Performing Organization Name and Address Lewis Research Center National Aeronautics and Space Administration Cleveland, Ohio 44135				8. Performing Organization Report No. E-6207	
12. Sponsoring Agency Name and Address National Aeronautics and Space Administration Washington, D. C. 20546				10. Work Unit No. 120-27	
15. Supplementary Notes				11. Contract or Grant No.	
16. Abstract <p>Experimental data are presented on subcooled and net-quality boiling heat transfer to water flowing vertically upward in tubes with uniform heat flux. Axial inner-wall-temperature distributions are tabulated for mass velocities from 0.67 to 141 kg/(sec)(m<sup>2</sup>), heat fluxes from 43.8 to 11 400 kW/m<sup>2</sup>, exit pressures from 24 to 690 kN/m<sup>2</sup> abs, exit qualities up to 0.65, and liquid subcoolings as high as 151 K. Since no satisfactory correlations are available for the full range of test conditions, these experimental data over a wide range of test conditions should be useful to the designer. It appears that, for low-quality and subcooled boiling, non-equilibrium effects must be taken into account, and no presently available model appears to be valid over the full range of subcooling.</p>				13. Type of Report and Period Covered Technical Note	
17. Key Words (Suggested by Author(s)) Boiler Heat transfer Nonequilibrium Subcooled boiling Net-quality boiling Experimental Correlations				14. Sponsoring Agency Code	
19. Security Classif. (of this report) Unclassified		18. Distribution Statement Unclassified - unlimited		15. Supplementary Notes	
20. Security Classif. (of this page) Unclassified		21. No. of Pages 37		22. Price* \$3.00	

# SUBCOOLED- AND NET-BOILING HEAT TRANSFER TO LOW-PRESSURE WATER IN ELECTRICALLY HEATED TUBES

by James R. Stone  
Lewis Research Center

## SUMMARY

Experimental data are presented on subcooled and net-quality boiling heat transfer to water flowing vertically upward in 0.584- and 1.219-centimeter inside diameter tubes with uniform heat flux. Axial inner-wall-temperature distributions are tabulated for mass velocities from 0.67 to 141 kg/(sec)(m<sup>2</sup>), heat fluxes from 43.8 to 11 400 kW/m<sup>2</sup>, exit pressures from 24 to 690 kN/m<sup>2</sup> abs, exit qualities up to 0.65, and liquid subcoolings as high as 151 K. Since no satisfactory correlations are available for the full range of test conditions, these experimental data over a wide range of test conditions should be useful to the designer.

The subcooled-boiling data are compared with some existing correlations. These correlations give the heat flux as a function of wall temperature minus saturation temperature. The data show only approximate agreement with the correlations, due probably to the effects of mass velocity, local subcooling, and distance from the inception of boiling. But the correlations are in the range of the data and may be useful for some applications.

Plots of net-boiling heat-transfer coefficients against quality do not agree with any existing correlation; the data show that, for constant heat flux, mass velocity, and quality, the local heat-transfer coefficient increases as pressure increases, whereas the correlations predict the opposite.

Heat-transfer coefficients, based on a wall-to-liquid temperature difference corrected for nonequilibrium, vary less with quality and show more consistent trends than do heat-transfer coefficients based on either wall-to-bulk or wall-to-saturation temperature differences. But no presently available nonequilibrium model appears to be valid over the entire range of liquid subcoolings of this study. Thus, a general heat-transfer correlation must be preceded by a nonequilibrium model valid for all subcoolings encountered.

## INTRODUCTION

An understanding of forced-flow boiling phenomena is necessary for the rational design of Rankine-cycle power systems, especially those for use in space, where compactness is important. Boiling, with its high heat-transfer coefficients, is also applicable to cooling problems where high heat fluxes are involved, such as in rocket-nozzle cooling. To obtain efficient, compact space power systems, high fluid temperatures are required. These high temperatures can be obtained at relatively low pressures by using alkali metals as working fluids. With the exception of liquid thermal conductivity, water has physical properties similar to the alkali metals. Since experiments on the boiling of alkali metals are difficult and expensive to perform, and since water itself may be of interest for cooling applications, a series of experiments on heat transfer and pressure drop for water boiling in tubes has been done at the NASA Lewis Research Center (refs. 1 to 5).

Although there have been numerous studies of boiling heat transfer, there is still no generally applicable means of prediction available for high-density-ratio fluids such as alkali metals and low-pressure water. This is especially true of the subcooled-boiling regime. Experimental results for high-heat-flux subcooled boiling of low-pressure water in 0.584-centimeter inside diameter tubes were presented in reference 1. In fully developed subcooled boiling, it was found that the wall temperature was nearly independent of fluid bulk temperature and mass velocity for a given pressure level and heat flux (the heat flux being in the range of about 1600 to 9100 kW/m<sup>2</sup>). Existing semiempirical correlations (refs. 6 to 8) did not satisfactorily predict the heat transfer at low pressures.

It is the objective of this study to obtain subcooled- and net-boiling heat-transfer data over a wide range of test variables, including the range covered in the heat-exchanger boiling studies (ref. 2). The range of interest is from the inception of boiling up to, but not including, the heat-transfer transition often called "burnout". This regime or series of regimes is often termed "nucleate boiling"; however, no such terminology is used herein since this range may include other regimes, such as evaporation from the interface with or without nucleation. The correlations of references 6 to 9 for subcooled-boiling heat transfer and references 10 to 14 for net-boiling heat transfer, based primarily on annular-flow models, are compared with the experimental data to determine whether or not any of them are applicable over the range of the experiments.

In order to obtain heat-transfer data under conditions comparable to those of the heat-exchanger boiling studies (ref. 2), the present heat-transfer studies employ 1.219- as well as 0.584-centimeter inside diameter tubes. The experimental test sections of this study are made of Inconel X tubing having a 0.025-centimeter-thick wall. The water flows vertically upward through the straight, circular tube. No inserts are used. Exit qualities as high as 0.65 are obtained.

## APPARATUS

Figure 1 shows a schematic diagram of the test apparatus. This is essentially the same test apparatus as that used in reference 1, wherein it is described in more detail. The system is designed to operate at a maximum pressure of  $1700 \text{ kN/m}^2$  abs and a maximum fluid temperature of 450 K.

The water is circulated by either of two gear pumps connected in parallel. The flow passes through the coiled stainless-steel electrical preheater to the test-section inlet plenum. From the exit plenum the flow passes through a 5.1-centimeter-diameter pipe to a spray condenser. The coolant is supplied to the condenser by a centrifugal pump having a nominal capacity of  $\sim 6.3 \times 10^{-3}$  cubic meter per second. From the condenser the flow passes into a multiple-tube heat exchanger cooled by cooling-tower water. In most cases the condenser is shut off, and the condensing is done in the heat exchanger.

The power to the test section and preheater is supplied by 70- and 250-kilowatt ac transformers, each regulated by a saturable core reactor. The two power supplies are interchangeable; either one can be connected to the test section or preheater, depending on the heat loads for a particular test.

## Test Sections

The test sections used in this investigation are constructed of 0.584- and 1.219-centimeter inside diameter by 0.25-millimeter wall Inconel X tubing and are from 14.6 to 121.9 centimeters long. This tubing is specially rolled to limit the wall-thickness deviation to less than 3 percent of the nominal wall thickness. The test-section inside-surface roughness is measured by a surface analyzer before and after use for a number of the test sections. The maximum surface roughness (peak to valley) is  $\sim 5$  nanometers. Several samples of tubing are used to measure the electrical resistivity of the Inconel X as a function of temperature. The results agree well with reference 15; the electrical resistivity of Inconel X may be considered independent of temperature for the range of this investigation.

Figure 2 shows a schematic diagram of a typical test section. The ratio of unheated length to inside diameter is 0.8 for test section 480-100M (table I) and 15 for all other test sections. (The test-section numbers give the inside diameter in thousandths of an inch followed by the ratio of heated length to inside diameter; the letter indicates the order of testing.) Power leads are connected to copper flanges that are silver-soldered to the tube. High temperature solder is used, and care is taken to ensure good contact and to avoid fillets in the heated portion of the test section. The end flanges are bolted

to the inlet and exit plenums and electrically insulated by Teflon and asbestos gaskets and seals. The exit plenum is fixed to the structural frame, while the inlet plenum is allowed to slide longitudinally to provide for thermal expansion. The test-section assembly is enclosed in a transparent shield to minimize external convective currents and to provide protection in case of failure.

## Instrumentation

Fluid temperatures. - Plenum chambers (fig. 3) are provided at the test-section inlet and exit in order to obtain (at least in the all-liquid case) true bulk-temperature readings. The inlet- and exit-plenum temperatures, as well as other fluid temperatures around the loop are measured by copper-constantan thermocouples and recorded by a multipoint self-balancing potentiometer. This instrument is periodically calibrated with a standard potentiometer. The error in the bulk temperatures is estimated to be  $\pm 0.3$  K.

Pressures. - For most of the data reported herein, the fluid pressures at the inlet and exit plenums are measured with strain-gage-type transducers having a range of 0 to  $690 \text{ kN/m}^2$  and a stated accuracy of 1/4 percent of full scale. The signal is recorded on a multichannel oscillograph. A 30-centimeter, 0- to  $690\text{-kN/m}^2$  Bourdon tube gage is connected to the exit plenum. In some cases, the test-section pressure drop is also measured with a 0- to  $207\text{-kN/m}^2$  differential gage connected across the pressure taps drilled through the copper flanges of the test section. Valves are provided to damp large amplitude gage pressure fluctuations or to shut off the gage completely. Under steady conditions, the correspondence between the transducers and gage readings is considered good.

Flow rate. - The flow rate is measured by one of three turbine-type flowmeters with overlapping ranges. All flowmeters are calibrated prior to their installation. The flowmeter signal is read from a frequency-converter indicator and on a digital frequency counter, both of which are calibrated by a signal generator.

Power. - Because a distorted ac output is obtained at low heating power levels (see ref. 1), a dynamometer-type wattmeter is used to measure the power input to the test section. The accuracy of this true rms instrument is 0.1 percent of full scale. A true rms, electronic-tube voltmeter is used to measure the test-section voltage drop and thus provide a check on the wattmeter.

Test-section wall temperatures. - The outside wall temperatures of the heated tube are measured by a number of 36-gage Chromel-Alumel thermocouples spot-welded in one longitudinal plane to the outside surface of the tube at various axial locations. The millivolt signal is recorded on a self-balancing potentiometer with a special filtering and isolation circuit to eliminate ac voltage pickup. Two 36-gage Chromel-Alumel thermo-

couples are spot-welded on the outside surface of the tube, both 0.635 centimeter from the exit end of the heated length, but circumferentially spaced  $180^\circ$  apart. These thermocouples are connected in parallel to yield a single average surface-temperature reading that is continuously recorded on a separate self-balancing potentiometer and serves as an overtemperature control.

## PROCEDURE

Prior to filling, the system is flushed with deionized water, purged with nitrogen, and then evacuated. It is then filled with deionized, deaerated water. The water is circulated through the system and further degassed by boiling in the test section and venting to the atmosphere from the top of the condenser. Generally, water samples are taken and analyzed daily on a gas analyzer for gas content. The dissolved gas content is maintained at or below 3 parts per million (by weight).

The desired conditions for each run are established by adjusting the power to the preheater and test section and setting the pump speed and system pressure at selected values. When the mean inlet and exit bulk temperatures become constant with time, the data for that run are taken. Temperatures are automatically recorded on strip charts. Flow rate, power, and pressures are read from gages.

In order to check the wall thermocouples, runs are made in which no heat is applied to the test section, but the flow rate and preheater power are varied. Since the heat losses are small, the tube-outer-wall temperatures can then be checked against the water bulk temperatures. The wall-temperature recorders are adjusted so that the bulk and wall temperatures agree within the scatter of the wall-temperature measurement.

## EXPERIMENTAL DATA

### Tabulation

The experimental heat-transfer data are presented in tables I to VII. For each run, the mass velocity, heat flux, inlet and exit temperatures, the inner-wall-temperature profile, the exit quality, exit pressure, and, when available, the test-section pressure drop are listed. Each wall-temperature reading is classified as nonboiling, subcooled boiling, or net boiling.

## Error Considerations

A maximum  $\pm 1.7$  K error in the inner-wall temperature is estimated in reference 1 for heat fluxes in excess of  $3150 \text{ kW/m}^2$ . This estimate is based on the maximum deviation in wall thickness, the accuracy of the outer-wall-temperature and heat-flux measurements, and the validity of the assumptions used in deriving the equation (1) for temperature drop through the heated wall. At the lower heat fluxes employed in the heat-transfer studies of this report, the errors should be less, perhaps in the vicinity of  $\pm 0.5$  K. Therefore, the wall temperatures are tabulated to the nearest 0.5 K. The error in the water temperature measurements is estimated to be  $\pm 0.3$  K (ref. 1); therefore, inlet and exit temperatures are tabulated to the nearest 0.1 K.

To estimate the heat loss from the test section, the heat-transfer coefficient to the air is estimated from reference 16, and the convective heat loss from the test-section surface is estimated to be less than 1 percent. Axial wall conduction calculations (ref. 17) based on measured temperature profiles indicate a maximum heat-transfer coefficient error of about 3 percent at the first measuring station, with error decreasing as length increases. During boiling, the rate of change of wall temperature with distance is usually quite small; thus, axial conduction is slight, and the assumptions used in deriving equation (1) for temperature drop through the wall are more valid.

## Data Reduction and Terminology

Figure 4 shows typical temperature and voidage profiles for the case of subcooling at the inlet and net quality at the exit and the pertinent terminology. The point of boiling initiation, as determined from the wall-temperature profile, is at  $z_o$ ; other parameters evaluated at this position are denoted by the subscript  $o$ . The subscript  $d$  denotes the point at which bubbles first detach from the tube wall. The point where the heat-balance quality is zero is indicated by the subscript  $1$ . Any quantity which is corrected for non-equilibrium is indicated by a superscript prime. (Symbols are defined in the appendix.)

The heat input is determined from the wattmeter. The comparison between the wattmeter reading and the power computed from the voltage measurement and the known test-section resistance agree well. The heat flux is computed by dividing the wattmeter power by the tube inside area over the length  $L_h$ . The outside wall temperature is obtained from the potentiometer millivolt signal by means of the calibrated temperature against emf curve for Chromel-Alumel thermocouples.

The inside wall temperature is computed as in references 1 and 17 by



$$0.593 (T_{wo} - T_w) + 0.000638 (T_{wo}^2 - T_w^2) = qD \left[ \frac{\ln\left(\frac{D_{wo}}{D}\right)}{1 - \left(\frac{D}{D_{wo}}\right)^2} - \frac{1}{2} \right] \quad (1)$$

which is derived for the following conditions: no heat loss from the outer surface, no axial heat flow within the wall, constant electrical resistivity, and a linear variation of thermal conductivity with temperature. Where the pressure drop is not determined experimentally, the pressure profiles are estimated using the correlations of references 18 and 2 for the subcooled- and net-boiling regimes, respectively. The liquid bulk temperature or vapor quality is then calculated by the following heat-balance equations, respectively:

$$T_\ell = T_i + \frac{4qz}{DGc_p} \quad (2)$$

$$x = \frac{4qz}{DG\lambda} - \frac{c_p}{\lambda} (T_s - T_i) \quad (3)$$

In comparing with net-boiling heat-transfer correlations, the fully developed all-liquid heat-transfer coefficient is required. The quantity  $(h_\ell D/k)(DG/\mu_\ell)^{-0.8}$  is given graphically as a function of Prandtl number  $c_p \mu_\ell / k$  in reference 17. Over the current range of interest, the relation for  $h_\ell$  may be approximated by

$$h_\ell = 0.0232 \left(\frac{k}{D}\right) \left(\frac{DG}{\mu_\ell}\right)^{0.8} \left(\frac{c_p \mu_\ell}{k}\right)^{0.467} \quad (4)$$

## RESULTS AND DISCUSSION

### Typical Data

Large subcooling at inlet. - Typical heat-transfer data with large subcooling ( $\sim 83$  K) at the inlet are shown in figure 5. Local inner-wall and bulk temperatures are plotted against the axial distance from the start of heating in figure 5(a). The bulk temperatures

are based on an equilibrium heat balance. The resulting local heat-transfer coefficients, based on bulk temperature, are plotted against distance in figure 5(b). Papell's correlation of subcooled-boiling heat transfer (ref. 9) is shown for comparison. Three runs are shown with variable heat flux and constant mass velocity, exit pressure, and inlet temperature.

At the lowest heat flux, the inner-wall temperature does not rise above saturation temperature until near the exit, and no boiling occurs. The local heat-transfer coefficient decreases with distance in the thermal entrance region and then increases slightly due to the effect of the increasing temperature on physical properties. For the intermediate heat flux, the inner-wall temperature rises with distance rapidly enough that subcooled boiling is initiated in the thermal entrance region; the heat-transfer coefficient then increases with distance throughout the rest of the tube, all in the subcooled-boiling regime. Qualitatively similar results are seen for the highest heat flux although boiling is initiated nearer the inlet, net vapor is produced (exit quality  $x_e = 0.044$ ), and the boiling heat-transfer coefficients are higher. It should be noted that, for both runs with boiling in figure 5(a), the inner-wall temperature increases with distance in the subcooled-boiling regime; this effect is not predicted by most subcooled-boiling heat-transfer correlations (e.g., refs. 6 to 8) but is of small magnitude. Throughout most of the subcooled-boiling regime, the experimental heat-transfer coefficients do not deviate greatly from Papell's correlation (ref. 9). But, the experimental data show less effect of distance (or subcooling) than predicted, and the deviation becomes large as the heat-balance quality approaches zero.

Small subcooling at inlet. - Typical heat-transfer data with small subcooling ( $\sim 22$  K) at the inlet are shown in figure 6; local inner-wall and bulk temperatures are plotted against axial distance from the start of heating in figure 6(a), and the resulting local heat-transfer coefficients, based on bulk temperature, are plotted against distance in figure 6(b). Papell's correlation of subcooled-boiling heat transfer (ref. 9) is again shown in figure 6(b) for comparison. Four runs are shown with variable heat flux and constant mass velocity and inlet temperature; the resulting exit quality ranges up to 0.247. The exit pressure is  $119 \text{ kN/m}^2$  abs at the lowest heat flux and increases by approximately  $7 \text{ kN/m}^2$  for each successive increase in heat flux; this increase in exit pressure is due to the increasing pressure drop between the boiler and condenser with increasing quality.

At the lowest heat flux, subcooled boiling is initiated somewhere near the middle of the tube, but the exact point is difficult to determine; the bulk condition at the exit is slightly subcooled. For the higher heat fluxes, subcooled boiling is initiated in the thermal entrance region, and net exit quality is produced. For all four runs, except very near the inlet, there is a general trend for inner-wall temperature to increase slightly with distance in the subcooled-boiling regime. For the three higher heat fluxes, at a

given position,  $h$  increases as  $q$  increases in the subcooled-boiling regime (fig. 6(b)). But then at a fairly low net quality,  $h$  takes on values of  $\sim 57 \text{ kW}/(\text{m}^2)(\text{K})$  and does not vary much with heat flux, distance, or quality. The agreement with Papell's correlation (ref. 9) is poorer here than for figure 5, especially for the lowest heat flux, indicating that the range of applicability of the correlation is limited to subcoolings on the order of 20 K or greater.

## Subcooled-Boiling Curves: Heat Flux Against Temperature Difference

A common way of presenting boiling heat-transfer data is to plot heat flux against wall superheat  $T_w - T_s$ . Figure 7 gives such a plot for an exit pressure of  $\sim 114 \text{ kN}/\text{m}^2$  abs; the data of this report and reference 1 as well as some limited data from reference 17 are shown. Two tube diameters and four length-to-diameter ratios are included. The wall-temperature measuring station 0.635-centimeter upstream of the test-section exit is used, except for the 1.219-centimeter inside diameter data of reference 17 where the station 1.905 centimeters upstream of the exit is used. Local subcooling  $T_s - T_\ell$  ranges from 3 to 66 K. The range of mass velocity is from 0.67 to 141  $\text{kg}/(\text{sec})(\text{m}^2)$ , while the heat-flux range is from 101 to 11 400  $\text{kW}/\text{m}^2$ . The correlations of Rohsenow (ref. 6), Forster and Greif (ref. 7), and Forster and Zuber (ref. 8) are shown for comparison. Although the data fall into a rather broad band ( $\sim 22 \text{ K}$ ) and cannot be said to agree with any correlation, the figure is useful in summarizing the range of results obtained. It may be that the effect of other variables, such as mass velocity and subcooling must be accounted for. The correlation of reference 8 gives approximately the lower limit of  $q$  for a given  $T_w - T_s$ . But it appears that the correlation of either reference 6 or 7 would give reasonable approximate results for many applications.

## Comparison With Net-Boiling Heat-Transfer Correlations

Most correlations of net-boiling heat-transfer coefficients relate  $h/h_\ell$  to the Martinelli parameter

$$X_{tt} = \left( \frac{1-x}{x} \right)^{0.9} \left( \frac{\rho_g}{\rho_\ell} \right)^{0.5} \left( \frac{\mu_g}{\mu_\ell} \right)^{0.1}$$

where  $h_\ell$  is the heat-transfer coefficient for all-liquid flow at saturation temperature. Figure 8 gives plots of  $h/h_\ell$  against  $x/(1-x)$  for mass velocities of  $\sim 0.68$  and  $\sim 5.9$

kg/(sec)(m<sup>2</sup>) at an exit pressure of ~117 kN/m<sup>2</sup> abs, from test section 480-100M (table I). Although some orderliness with regard to heat flux can be seen in both figures, it is apparent that the effect of mass velocity is not properly accounted for. The correlation of Dengler and Addoms (ref. 10) is shown for comparison. Although the data are not in agreement with the correlation, the slope of  $h/h_\ell$  against  $x/(1-x)$  appears to agree for relatively high qualities in figure 8(a).

Similar plots are shown in figure 9 for a mass velocity of ~0.68 kg/(sec)(m<sup>2</sup>) at exit pressures of ~114 and ~26 kN/m<sup>2</sup> abs, from test section 480-50M (table II). The data of figures 8(a) and 9(a) show good agreement between the two test sections. But the experimental data show that, for constant heat flux, mass velocity, and quality,  $h/h_\ell$  (and also  $h$ ) increases as pressure increases, whereas the correlation of reference 10 (and also those of refs. 11 to 14) predicts the opposite, due to the physical properties in  $X_{tt}$ . Although the correlations of references 10 and 14 include a nucleate-boiling term, which is not directly a function of  $X_{tt}$ , the contribution of the nucleate term is not of sufficient magnitude to reverse the pressure effect in either case. Thus these correlations in terms of  $X_{tt}$  are inadequate.

## Definition of Heat-Transfer Coefficient During Boiling

In net boiling (equilibrium heat-balance quality  $x > 0$ ) the heat-transfer coefficient is usually defined as  $q/(T_w - T_s)$ , while in the subcooled-boiling regime, either  $q/(T_w - T_s)$  or  $q/(T_w - T_\ell)$  is commonly used. In figures 5(b) and 6(b) the latter definition,  $h = q/(T_w - T_\ell)$ , is used with  $T_\ell = T_s$  for  $x > 0$ . These heat-transfer coefficients are plotted against local equilibrium heat-balance quality  $x$  in figure 10(a). It can be seen that  $h$  increases rapidly with  $x$  in the subcooled region ( $x < 0$ ) and passes through a maximum in the low-quality range. In figure 10(b),  $h_s = q/(T_w - T_s)$  is plotted against  $x$  for these same runs. It is difficult to find any consistent trends. These two definitions of the heat-transfer coefficient are not the only ones possible, however. Since some of the heat added to a fluid in subcooled boiling goes into the production of vapor, the remaining liquid has a lower average temperature  $T'_\ell$  than that calculated from an equilibrium heat balance. Performing a heat balance from the point of boiling initiation (subscript  $o$ ) to any downstream point,

$$T'_\ell = T_{\ell, o} + \frac{4q(z - z_o)}{DGc_p} \left( \frac{1 - \bar{\gamma}}{1 - x'} \right) \quad (5)$$

where  $x'$  is the actual quality and  $\bar{\gamma}$  is the net fraction of the heat added from  $z_o$  to  $z$

going into vaporization  $x'/(x - x_0)$ . There are several means available for predicting  $x'$  and  $\bar{\gamma}$ ; for the present discussion, the following simple relation suggested by Levy (ref. 19) is used:

$$x' = x - x_d e^{(x/x_d)-1} \quad (6)$$

where  $x_d$  is the equilibrium heat-balance quality at the point where bubbles first depart from the surface; hereinafter,  $x_d$  is taken to be  $x_0$ . The heat-transfer coefficient corrected for nonequilibrium,  $h' = q/(T_w - T'_l)$  is plotted against the equilibrium heat-balance quality  $x$  in figure 10(c). It can be seen that the range of  $h'$  values is much less than that of  $h$  or  $h_s$ , and the variation of  $h'$  with  $x$  is less than that of  $h$  or  $h_s$ .

Another reasonable plot to make is  $h'$  against  $x'$ ; this is shown in figure 11. In both figures 10(c) and 11 there is an apparent effect of inlet temperature; other relations, suggested by Kroeger and Zuber (ref. 20), give similar results. This may be due in part to the contribution of nucleate boiling; but neither of the correlations (that of ref. 10 or 14), using nonequilibrium quality, agree well with the data. However, it should be noted that equation (6) is an assumed equation, used previously only for smaller subcoolings, and the assumption that  $x_0 = x_d$  may contribute to the apparent subcooling effect. It appears that  $x'$  is calculated to be too large; pressure drop calculations also indicate that  $x'$  is too large. Therefore, although it might be possible to obtain  $h'$  as a function of  $x$  or  $x'$ ,  $q$ ,  $G$ , and physical property values for a given initial subcooling, it appears that a nonequilibrium model valid over a wide range of subcooling and pressure is still required before a general correlation of the data will be successful.

## SUMMARY OF RESULTS

The major results of this investigation of heat transfer to low-pressure water in subcooled and net-quality boiling in electrically heated tubes may be summarized as follows:

1. Axial inner-wall temperature distributions are tabulated for subcooled and net boiling in 0.584- and 1.219-centimeter inside diameter tubes over the following ranges of test variables: mass velocity from 0.67 to 141 kg/(sec)(m<sup>2</sup>), heat flux from 43.8 to 11 400 kW/m<sup>2</sup>, exit pressure from 24 to 690 kN/m<sup>2</sup> abs, qualities up to 0.65, and liquid subcoolings as high as 151 K. As no satisfactory general correlations are available, these experimental data over a wide range of test conditions should be useful to the designer.

2. The subcooled-boiling data show only approximate agreement with the correlations of Rohsenow, Forster and Greif, Forster and Zuber, and Papell. In some cases the

tube-inner-wall temperature increases with increasing distance from the start of heating in the subcooled-boiling regime, which is not predicted by any existing correlation; however, this effect is small.

3. Plots of net-boiling heat-transfer coefficients against heat-balance quality do not agree with any existing correlation; the data show that, for constant heat flux, mass velocity, and quality, the local heat-transfer coefficient increases as pressure increases whereas the correlations predict the opposite.

4. Heat-transfer coefficients, based on a wall-to-liquid temperature difference corrected for nonequilibrium, vary less with quality and show more consistent trends than do heat-transfer coefficients based on either wall-to-bulk or wall-to-saturation temperature differences. However, a completely satisfactory correlation of the data is not attained because no presently available nonequilibrium model appears to be valid over the entire range of liquid subcoolings of this study.

Lewis Research Center,  
National Aeronautics and Space Administration,  
Cleveland, Ohio, April 1, 1971,  
120-27.

## APPENDIX - SYMBOLS

$c_p$	liquid heat capacity, J/(kg)(K)
$D$	tube inside diameter, m
$D_{wo}$	tube outside diameter, m
$G$	mass velocity, kg/(sec)(m <sup>2</sup> )
$h$	heat-transfer coefficient, $q/(T_w - T_\ell)$ , W/(m <sup>2</sup> )(K)
$h_\ell$	calculated all-liquid heat-transfer coefficient (eq. (4)), W/(m <sup>2</sup> )(K)
$h_s$	boiling heat-transfer coefficient, $q/(T_w - T_s)$ , W/(m <sup>2</sup> )(K)
$k$	liquid thermal conductivity, W/(m)(K)
$L_h$	heated length of test section, m
$L_u$	unheated length of test section, m
$P$	pressure, N/m <sup>2</sup> abs
$\Delta P$	test-section pressure drop, N/m <sup>2</sup>
$q$	heat flux, W/m <sup>2</sup>
$T$	temperature, K
$X_{tt}$	Martinelli parameter, $\left(\frac{1-x}{x}\right)^{0.9} \left(\frac{\rho_g}{\rho_\ell}\right)^{0.5} \left(\frac{\mu_g}{\mu_\ell}\right)^{0.1}$ , dimensionless
$x$	vapor quality (eq. (3)), dimensionless
$z$	axial distance from start of heating, m
$\bar{\gamma}$	fraction of heat added going into vaporization, $x'/(x - x_o)$ , dimensionless
$\lambda$	enthalpy of vaporization, J/kg
$\mu$	viscosity, kg/(sec)(m)
$\rho$	density, kg/m <sup>3</sup>
Subscripts:	
$d$	point where bubbles first detach from tube wall
$e$	test-section exit
$g$	gas property
$i$	test-section inlet
$\ell$	liquid property, or based on liquid bulk temperature

- o onset of boiling, as determined from wall-temperature profile
- s saturation, or based on saturation temperature
- w tube inner wall
- wo tube outer wall
- 1 point where heat-balance quality is zero

Superscript:

- ' value corrected for nonequilibrium

## REFERENCES

1. Jeglic, Frank A.; Stone, James R.; and Gray, Vernon H.: Experimental Study of Subcooled Nucleate Boiling of Water Flowing in 1/4-Inch-Diameter Tubes at Low Pressures. NASA TN D-2626, 1965.
2. Stone, James R.; and Damman, Thomas M.: An Experimental Investigation of Pressure Drop and Heat Transfer for Water Boiling in a Vertical-Upflow Single-Tube Heat Exchanger. NASA TN D-4057, 1967.
3. Stone, James R.; and Sekas, Nick J.: Tests of a Single Tube-in-Shell Water-Boiling Heat Exchanger With a Helical-Wire Insert and Several Inlet Flow-Stabilizing Devices. NASA TN D-4767, 1968.
4. Stone, James R.; and Sekas, Nick J.: Tests of a Single-Tube-in-Shell Water Boiler With Helical-Wire Insert, Inlet Nozzle, and Two Different Inlet-Region Plugs. NASA TN D-5644, 1970.
5. Sekas, Nick J.; and Stone, James R.: Experimental Study of Blade-Type Helical Flow Inducers in a 5/8-Inch Electrically Heated Boiler Tube. NASA TM X-2001, 1970.
6. Rohsenow, Warren M.: Heat Transfer Associated with Nucleate Boiling. Heat Transfer and Fluid Mechanics Institute, Stanford Univ. Press, 1953, pp. 123-141.
7. Engelberg-Forster, Kurt; and Greif, R.: Heat Transfer to a Boiling Liquid-Mechanism and Correlations. J. Heat Transfer, vol. 81, no. 1, Feb. 1959, pp. 43-53.
8. Forster, H. K.; and Zuber, N.: Dynamics of Vapor Bubbles and Boiling Heat Transfer. AIChE J., vol. 1, no. 4, Dec. 1955, pp. 531-535.
9. Papell, S. Stephen: Subcooled Boiling Heat Transfer Under Forced Convection in a Heated Tube. NASA TN D-1583, 1963.



10. Dengler, C. E.; and Addoms, J. N.: Heat Transfer Mechanism for Vaporization of Water in a Vertical Tube. Chem. Eng. Prog. Symp. Ser., vol. 52, no. 18, 1956, pp. 95-103.
11. Wright, Roger M.: Downflow Forced-Convection Boiling of Water in Uniformly Heated Tubes. Rep. UCRL-9744, Univ. California, Lawrence Radiation Lab., Aug. 21, 1961.
12. Schrock, V. E.; and Grossman, L. M.: Forced Convection Boiling Studies. Univ. California, Lawrence Radiation Lab. (AEC Rep. TID-14632), Nov. 1, 1959.
13. Collier, J. G.; and Pulling, D. J.: Heat Transfer to Two-Phase Gas-Liquid Systems. Part II: Further Data on Steam-Water Mixtures. Rep. AERE-R-3809, United Kingdom Atomic Energy Authority, 1962.
14. Chen, John C.: A Correlation for Boiling Heat Transfer to Saturated Fluids in Convective Flow. Paper 63-HT-34, ASME, 1963.
15. Anon.: Engineering Properties of Inconel and Inconel X. Tech. Bull. T-7, International Nickel Co., Sept. 1959.
16. Kreith, Frank: Principles of Heat Transfer. International Textbook Co., 1958.
17. Stone, James R.: Local Turbulent Heat Transfer for Water in Entrance Regions of Tubes with Various Unheated Starting Lengths. NASA TN D-3098, 1965.
18. Stone, James R.: A Correlation of Subcooled-Boiling Pressure Drop for Low-Pressure Water Flowing in Tubes with Constant Heat Flux. Presented at the 63rd Annual AIChE Meeting, Chicago, Ill., paper 48f, Nov. 29-Dec. 3, 1970.
19. Levy, S.: Forced Convection Subcooled Boiling-Prediction of Vapor Volumetric Fraction. Int. J. Heat Mass Transfer, vol. 10, no. 7, July 1967, pp. 951-965.
20. Kroeger, P. G.; and Zuber, N.: An Analysis of the Effects of Various Parameters on the Average Void Fractions in Subcooled Boiling. Int. J. Heat Mass Transfer, vol. 11, no. 2, Feb. 1968, pp. 211-233.



49	2.36	107	357.6	375.1	123	.038	a377.0	b376.0	b381.0	b388.0	b386.0	b387.0	b385.5	b384.0	b384.0	b383.0	b382.0	b382.5	b383.0	b383.0	b383.0	b383.0	b383.0	b383.0	b383.0	b383.0	b383.0	b383.0
50	2.38	134	358.2	374.8	123	.062	a379.0	a386.0	a390.0	a384.5	a387.0	a387.0	a386.0	a387.0	a386.0	a386.0	a386.0	a387.0	a387.0	a387.0	a387.0	a387.0	a386.0	a386.0	a386.0	a386.0	a386.0	a386.0
51	2.39	163	355.9	374.3	123	.079	a379.5	a388.0	a386.0	a382.5	a385.0	a384.0	a384.0	a384.0	a384.0	a384.0	a385.0	a385.0	a385.0	a385.0	a385.0	a385.0	a385.0	a385.0	a385.0	a385.0	a385.0	a385.0
52	2.35	199	357.6	373.7	d127	.112	a384.0	a385.0	a383.0	a384.0	a386.0	a384.0	a384.0	a384.0	a384.0	a384.0	a385.0	a385.0	a385.0	a385.0	a385.0	a385.0	a385.0	a385.0	a385.0	a385.0	a385.0	a385.0
53	2.34	231	356.5	374.3	d123	.135	a383.0	a386.5	a384.0	a384.0	a385.5	a384.0	a384.0	a384.0	a384.0	a384.0	a385.0	a385.0	a385.0	a385.0	a385.0	a385.0	a385.0	a385.0	a385.0	a385.0	a385.0	a385.0
54	2.34	284	357.1	373.7	d123	.178	a382.5	a388.0	a385.0	a384.5	a386.0	a384.5	a384.0	a387.0	a385.0	a386.0	a386.0	a386.0	a386.0	a386.0	a386.0	a386.0	a386.0	a386.0	a386.0	a386.0	a386.0	a386.0
55	1.39	64	359.8	375.7	119	.088	a371.0	a378.0	a383.5	a388.0	a387.0	a388.0	a385.0	a384.0	a382.0	a381.0	a382.0	a382.0	a382.0	a382.0	a382.0	a382.0	a382.0	a382.0	a382.0	a382.0	a382.0	a382.0
56	1.39	91	366.4	375.1	119	.085	a377.0	a386.0	a384.0	a384.0	a388.0	a385.0	a384.0	a382.5	a383.0	a383.0	a383.0	a383.0	a383.0	a383.0	a383.0	a383.0	a383.0	a383.0	a383.0	a383.0	a383.0	a383.0
57	0.69	44	355.9	373.2	117	.073	a367.5	a374.0	a380.0	a386.0	a383.0	a383.0	a382.5	a380.5	a378.0	a379.0	a378.0	a379.0	a379.5	a380.0	a380.0	a380.0	a380.0	a380.0	a380.0	a380.0	a380.0	a380.0
58	0.69	63	354.8	375.4	123	.118	a375.0	a361.5	a389.0	a386.5	a384.0	a384.0	a382.0	a380.0	a381.0	a381.0	a381.0	a381.0	a382.0	a382.0	a382.0	a382.0	a382.0	a382.0	a382.0	a382.0	a382.0	a382.0
59	0.69	79	354.3	375.1	123	.158	a380.0	a388.0	a384.5	a384.0	a384.0	a383.0	a383.0	a380.0	a381.0	a382.0	a382.0	a382.0	a383.0	a383.0	a383.0	a383.0	a383.0	a383.0	a383.0	a383.0	a383.0	a383.0
60	0.70	103	354.3	375.1	123	.218	a386.0	a391.0	a383.0	a384.0	a395.0	a383.0	a383.0	a383.0	a383.0	a385.0	a385.0	a385.0	a385.0	a385.0	a385.0	a385.0	a385.0	a385.0	a385.0	a385.0	a385.0	a385.0
61	0.68	127	357.1	375.1	d123	.295	a386.0	a384.0	a382.5	a383.0	a383.0	a382.0	a384.0	a384.0	a386.0	a386.0	a386.0	a386.0	a386.0	a386.0	a386.0	a386.0	a386.0	a386.0	a386.0	a386.0	a386.0	a386.0
62	0.69	155	355.4	374.4	d123	.357	a385.0	a385.0	a382.0	a381.0	a382.0	a385.0	a385.0	a385.0	a386.0	a386.0	a386.0	a386.0	a386.0	a386.0	a386.0	a386.0	a386.0	a386.0	a386.0	a386.0	a386.0	a386.0
63	0.69	198	356.5	375.1	d123	.491	a381.0	a385.0	a381.0	a379.0	a382.0	a385.0	a386.0	a386.0	a386.0	a386.0	a386.0	a386.0	a386.0	a386.0	a386.0	a386.0	a386.0	a386.0	a386.0	a386.0	a386.0	a386.0
64	0.69	234	357.1	375.1	d123	.570	a381.5	a395.0	a381.0	a378.5	a383.0	a380.0	a385.0	a387.0	a384.0	a387.0	a387.0	a387.0	a388.0	a388.0	a388.0	a388.0	a388.0	a388.0	a388.0	a388.0	a388.0	a388.0
65	0.69	269	355.9	374.8	d123	.652	(b)	(b)	(b)	(b)	(c)	(c)	(c)	(c)	(c)	(c)	(c)	(c)	(c)	(c)	(c)	(c)	(c)	(c)	(c)	(c)	(c)	(c)
2	1.34	160	298.7	363.7	99	---	a329.5	a339.0	a349.0	a356.0	a373.0	a379.0	a376.0	a376.5	a376.5	a382.0	a379.0	a378.0	a378.0	a380.0	a380.0	a382.0	a382.0	a382.0	a382.0	a382.0	a382.0	a382.0
3	1.00	100	293.7	370.4	99	.032	a334.5	a343.0	a354.0	a368.0	a378.0	a376.0	a376.5	a380.0	a381.0	a382.0	a380.0	a380.0	a380.0	a382.0	a380.0	a380.5	(c)	a383.0	a379.0	(c)	a383.0	a379.0
4	0.69	94	294.3	377.6	122	.099	a339.5	a349.5	a360.0	a370.0	a385.0	a384.0	a383.0	a379.0	a384.0	a384.0	a386.0	a386.0	a386.0	a385.0	a385.0	a385.0	(c)	a386.0	a386.0	a386.0	a386.0	a386.0
5	1.36	130	293.2	373.7	108	.017	a338.0	a349.0	a362.0	a377.0	a381.0	a378.5	a381.0	a377.0	a383.0	a384.5	a383.0	a377.0	a382.0	a384.0	a384.0	a383.0	(b)	a385.0	a380.0	(b)	a385.0	a380.0
6	1.00	131	293.2	378.7	126	.074	a345.0	a356.0	a369.0	a383.0	a380.5	a384.5	a384.5	a383.0	a387.0	a389.0	a387.5	a378.5	a387.0	a385.0	a386.0	a387.5	(b)	a387.5	a388.0	(b)	a387.5	a388.0
7	1.34	132	292.6	373.7	d110	.020	a341.0	a351.0	a364.5	a374.0	a382.0	a384.0	a378.0	a383.0	a384.0	a384.0	a384.0	a382.5	a383.0	a383.5	a385.0	a385.0	(b)	a387.0	a383.0	(b)	a387.0	a383.0
8	1.00	132	293.2	375.4	114	.079	a346.0	a358.5	a371.0	a385.0	a380.0	a381.0	a381.0	a381.0	a383.0	a386.0	a385.5	a385.5	a384.0	a384.0	a385.0	a386.0	(c)	a389.0	a383.0	(c)	a389.0	a383.0
9	0.69	136	293.2	375.0	118	.178	a351.0	a362.5	a376.0	a389.0	a380.0	a382.0	a385.5	a386.0	a385.5	a385.5	a386.0	a384.0	a386.0	a386.0	a385.5	a386.0	(c)	a389.0	a385.0	(c)	a389.0	a385.0
13	2.36	193	295.9	372.1	112	---	a348.0	a360.0	a371.5	a381.5	a384.0	a385.0	a387.0	a387.0	a387.0	a387.0	a387.0	a387.0	a387.0	a387.0	a387.0	a387.0	(b)	a390.0	a387.0	(b)	a390.0	a387.0
14	1.34	192	296.5	374.3	117	.106	a362.0	a375.0	a388.0	a383.0	a384.0	a386.0	a386.0	a388.0	a388.0	a389.0	a387.0	a387.0	a387.0	a387.0	a387.0	a388.0	(c)	a391.0	a389.0	(c)	a391.0	a389.0
15	1.00	190	296.5	374.3	119	.187	a368.0	a382.0	a387.0	a385.0	a385.5	a387.0	a387.0	a389.0	a389.0	a387.0	a384.5	a386.0	a387.0	a387.5	a389.0	a389.0	(c)	a392.0	a389.0	(c)	a392.0	a389.0
16	0.69	196	296.5	374.3	119	.348	a375.0	a389.0	a387.0	a383.0	a385.5	a388.0	a387.0	a386.0	a385.0	a386.0	a386.0	a386.0	a387.5	a388.0	a390.0	a390.0	(c)	a392.0	a389.0	(c)	a392.0	a389.0
17	4.63	252	295.4	347.1	112	---	a335.0	a346.0	a352.0	a360.0	a374.0	a371.5	a375.0	a377.0	a376.0	a378.5	a378.5	a378.5	a378.5	a379.5	a381.0	a382.5	(b)	a391.0	a387.0	(b)	a391.0	a387.0
18	2.37	251	297.6	374.3	118	.041	a362.0	a378.0	a383.0	a382.0	a384.0	a385.0	a385.0	a387.0	a388.0	a385.0	a389.0	a389.0	a389.0	a389.0	a389.0	a389.0	(c)	a392.0	a389.0	(c)	a392.0	a389.0
19	1.34	251	296.5	374.3	117	.184	a383.0	a389.0	a388.0	a383.0	a386.5	a387.0	a388.0	a388.0	a388.0	a387.5	a388.5	a388.5	a387.5	a387.5	a391.0	a391.0	(c)	a392.0	a389.0	(c)	a392.0	a389.0

<sup>a</sup>Nonboiling.

<sup>b</sup>Subcooled boiling.

<sup>c</sup>Net-quality boiling.

<sup>d</sup>Pressure oscillation of  $>3.5 \text{ kN/m}^2$ .

<sup>e</sup>Rose to 397 K causing automatic shutdown.

TABLE II. - HEAT-TRANSFER DATA FOR 1.219-CENTIMETER INSIDE DIAMETER BY 61-CENTIMETER-LONG TEST SECTION 480-50 M

[G = mass velocity, kg/(sec)(m<sup>2</sup>); q = heat flux, kW/m<sup>2</sup>; T<sub>i</sub> = inlet temperature, K; T<sub>e</sub> = exit temperature, K; P<sub>e</sub> = exit pressure, kN/m<sup>2</sup> abs; x<sub>e</sub> = exit quality.]

Run	G	q	T <sub>i</sub>	T <sub>e</sub>	P <sub>e</sub>	x <sub>e</sub>	Axial distance from start of heating, z, cm															
							0.635	1.270	2.540	5.080	10.16	15.24	20.32	25.40	30.48	35.56	40.64	45.72	50.80	55.88	60.32	
							Inner-wall temperature, T <sub>w</sub> , K															
17	5.89	253	294.8	314.8	110	----	a335.0	a343.0	a354.0	a355.0	a365.0	a370.0	a372.0	a375.0	a376.0	a377.0	a377.0	a378.0	a379.5	b380.0	b377.0	
18	5.91	315	294.8	320.9	110	----	a345.0	a354.0	a363.0	a370.0	a375.0	a376.5	a376.5	a378.0	a379.0	a379.0	a379.0	a380.0	a379.0	b379.0	b380.0	
19	5.92	192	323.7	338.7	110	----	a347.0	a353.0	a360.0	a361.0	a364.0	a368.0	a369.0	a370.0	a373.0	a374.0	a375.0	a376.0	a378.0	a378.0	a378.0	
20	5.92	258	324.0	344.6	110	----	a356.5	a363.0	a368.0	a375.0	a376.5	a377.0	a379.0	a379.0	b379.0	b379.0	b379.0	b381.0	b379.0	b380.0	a379.0	
21	5.89	328	324.0	350.4	110	----	a366.5	a373.0	a375.0	b378.0	b375.0	b378.0	b379.0	b378.0	b379.0	b380.0	b379.0	b378.0	b380.5	b386.5	b385.0	
13	2.38	126	295.9	321.5	107	----	a333.0	a344.0	a353.0	a366.5	b374.0	b379.0	b379.0	b379.0	b379.0	b381.0	b379.0	b379.0	b382.0	b382.0	b379.0	
14	2.38	192	295.4	333.2	110	----	a352.0	a363.0	b376.0	b376.0	b374.0	b376.0	b376.0	b374.0	b376.5	b375.0	b375.0	b377.0	b378.0	b377.0	b376.5	
15	2.38	254	294.8	345.9	110	----	a367.0	b380.0	b377.0	b380.0	b380.0	b377.0	b383.0	b384.0	b384.0	b384.0	b384.0	b385.0	b385.5	b386.5	b385.0	
16	2.38	322	294.8	358.7	110	----	a376.5	b380.0	b380.0	b380.0	b380.0	b384.0	b384.0	b384.0	b385.0	b385.0	b385.0	b386.0	b386.0	b385.0	b385.0	
22	2.38	103	320.9	340.9	110	----	a347.0	a354.0	a361.0	a367.0	a373.0	b381.5	b374.0	b375.0	b374.0	b376.0	b376.5	b376.5	b378.0	b375.0	b374.0	
23	2.38	128	320.9	345.9	110	----	a354.0	a361.5	a370.0	b376.5	b374.0	b375.0	b377.0	b375.0	b378.0	b378.0	b378.0	b378.0	b378.0	b378.0	b375.0	
24	2.38	192	320.7	358.7	110	----	a369.0	a380.0	b381.0	b381.5	b381.5	b383.0	b383.0	b384.0	b384.0	b384.0	b384.0	b384.0	b384.5	b384.0	b386.5	
25	2.38	258	320.4	371.5	110	----	b383.0	b381.0	b375.0	b375.0	b379.0	b382.0	b382.0	b385.0	b385.0	b385.0	b385.0	b386.0	b386.0	b386.0	b384.0	
26	2.38	315	320.4	374.3	109	-0.16	b385.0	b385.0	b385.0	b385.0	b384.0	b386.5	b385.0	b385.0	b385.0	b385.0	b385.0	b385.0	b385.5	b385.0	b385.0	
37	2.38	102	344.3	364.3	98	----	a363.0	a370.0	a376.5	b381.0	b379.0	b381.0	b380.0	b380.0	b380.0	b380.0	b380.0	b380.0	b380.0	b380.0	b378.0	
38	2.38	119	345.4	368.7	98	----	a369.0	a376.0	a378.0	b379.0	b378.0	b380.0	b380.0	b380.0	b380.0	b380.0	b380.0	b380.0	b380.0	b379.0	b379.0	
39	2.38	198	345.4	374.3	108	0.19	b385.0	b384.0	b382.0	b384.0	b381.0	b384.0	b383.0	b383.0	b383.0	b383.0	b383.0	b383.0	b384.0	b384.0	b384.0	
6	0.68	54	298.2	335.4	109	----	a327.0	a333.0	a342.0	a350.0	a360.0	a366.5	a371.0	a371.5	a374.0	a358.0	a361.0	a367.0	a374.5	a376.5	a376.5	
7	0.68	101	297.1	346.8	109	----	a346.5	a358.0	a370.0	b379.0	b379.0	b380.0	b381.5	b381.5	b383.0	b381.5	b381.5	b383.0	b381.5	b382.0	b382.0	
8	0.68	124	297.1	373.2	109	-0.14	a355.0	a356.5	a379.0	b379.0	b381.0	b382.0	b383.0	b383.0	b383.0	b383.0	b383.0	b383.0	b383.0	b383.0	b383.0	
9	0.68	154	297.1	373.2	108	-0.55	a368.0	b381.5	b381.5	b381.0	b380.0	b379.0	b383.0	b383.0	b383.0	b383.0	b383.0	b383.0	b383.0	b383.0	b383.0	
10	0.68	191	298.7	375.4	114	-1.05	b378.0	b378.0	b379.0	b380.0	b380.0	b384.0	b383.0	b383.0	b383.0	b384.0	b384.0	b384.0	b385.0	b385.0	b385.0	
11	0.69	259	298.2	375.4	114	-1.91	b384.0	b384.0	b383.0	b384.0	b382.0	b385.0	b383.0	b383.0	b384.0	b383.0	b385.0	b385.0	b385.0	b385.0	b386.5	
12	0.69	315	297.6	374.8	114	-2.62	b384.0	b384.0	b383.0	b384.0	b382.0	b384.0	b383.0	b383.0	b384.0	b385.0	b385.0	b385.0	b386.5	b386.5	b386.5	
27	0.71	105	336.5	374.3	108	0.61	a379.0	b386.5	b383.0	b383.0	b383.0	b384.0	b384.0	b384.0	b383.0	b383.0	b384.0	b384.0	b385.0	b384.0	b384.0	
28	0.69	185	326.5	376.5	117	-1.43	b388.0	b386.5	b384.0	b384.0	b385.0	b384.0	b386.5	b384.0	b385.0	b386.0	b386.0	b386.0	b386.5	b386.5	b386.5	
29	0.69	256	325.4	376.5	116	-2.34	b386.0	b385.0	b385.0	b386.0	b383.0	b385.0	b385.0	b386.0	b386.0	b387.0	b387.0	b387.0	b388.0	b388.0	b386.5	
30	0.69	322	325.4	375.9	114	-3.22	b386.0	b385.0	b385.0	b386.0	b382.0	b385.0	b385.0	b385.0	b386.5	b388.0	b388.0	b389.0	b389.0	b390.0	b391.0	
31	0.69	126	348.7	375.4	112	-1.11	b386.0	b384.0	b384.0	b384.0	b382.0	b384.0	b383.0	b385.0	b385.0	b385.0	b385.0	b385.0	b385.0	b386.5	b386.0	
32	0.69	191	349.8	375.9	113	-1.98	b386.5	b385.0	b385.0	b384.0	b382.0	b384.0	b385.0	b385.0	b385.0	b384.0	b384.0	b388.0	b387.0	b388.0	b387.0	
33	0.68	254	348.7	375.9	112	-2.83	b386.0	b386.0	b383.0	b383.0	b381.5	b385.0	b385.0	b385.0	b386.0	b386.0	b387.0	b388.0	b388.0	b388.0	b388.0	
34	0.69	325	350.9	375.9	112	-3.69	b385.0	b385.0	b383.0	b383.0	b382.0	b385.0	b385.0	b385.0	b385.0	b389.0	b389.0	b389.0	b390.5	b390.0	b390.0	
41	0.69	97	295.9	338.4		d <sub>26</sub>	0.045	(e)	(e)	(e)	(e)	(e)	(e)	(e)	b350.0	b349.0	b348.0	b348.0	b350.0	b350.0	b347.0	
42	0.69	126	295.9	338.2		d <sub>25</sub>	0.082	(e)	(e)	(e)	(e)	(e)	(e)	(e)	b351.5	b349.0	b348.0	b350.0	b351.5	b353.0	b349.0	
43	0.69	193	295.4	338.2		d <sub>25</sub>	0.164	(e)	(e)	(e)	(e)	(e)	(e)	(e)	b350.0	b351.5	b348.0	b350.0	b351.5	b353.0	b353.0	
44	0.69	254	295.4	338.2		d <sub>25</sub>	0.241	(g)	(g)	(g)	(g)	(g)	(g)	(g)	(g)	(g)	(g)	(g)	(g)	(g)	(g)	b355.0
45	0.69	108	335.9	338.7		d <sub>26</sub>	-1.29	a348.0	a349.0	b351.0	b350.0	b351.0	b350.0	b354.0	b352.0	b355.0	b354.0	b357.0	b357.0	b357.0	b354.0	b352.0
46	0.69	127	335.4	338.7		d <sub>26</sub>	-1.52	b352.0	b350.0	b351.5	b351.5	b352.0	b354.0	b355.0	b356.5	b356.5	b357.0	b357.0	b357.0	b357.0	b356.5	b355.0
47	0.69	194	334.8	339.3		d <sub>26</sub>	-2.34	b353.0	b353.0	b354.0	b356.0	b359.0	b359.0	b358.0	b360.0	b358.0	b360.0	b360.0	b359.0	b359.0	b358.0	b353.0
48	0.69	256	335.4	339.3		d <sub>26</sub>	-3.14	b352.0	b352.0	b352.0	b353.0	b352.0	b355.0	b356.5	b357.0	b356.0	b359.0	b359.0	b358.0	b358.0	b356.5	b352.0

<sup>a</sup>Nonboiling.

<sup>b</sup>Subcooled boiling.

<sup>c</sup>Net-quality boiling.

<sup>d</sup>Estimated from exit temperature.

<sup>e</sup>Very unsteady.

<sup>f</sup>Temperature oscillation.

<sup>g</sup>Automatic shutdown did not allow measurement.

<sup>h</sup>Automatic shutdown after data taken.

TABLE III. - HEAT-TRANSFER DATA FOR 1.219-CENTIMETER INSIDE DIAMETER BY 61-CENTIMETER-LONG TEST SECTION 480-50

[G = mass velocity, kg (sec)(m<sup>2</sup>); q - heat flux, kW m<sup>-2</sup>; T<sub>1</sub> - inlet temperature, K; T<sub>e</sub> = exit temperature, K; P<sub>e</sub> = exit pressure, kN/m<sup>2</sup> abs; x<sub>e</sub> = exit quality; ΔP = pressure drop, kN m<sup>-2</sup>.]

Run	G	q	T <sub>1</sub>	T <sub>e</sub>	P <sub>e</sub>	x <sub>e</sub>	ΔP	Axial distance from start of heating, z, cm															
								2.540	7.645	12.70	17.78	22.89	27.94	33.02	38.10	43.18	48.26	53.34	58.42	59.05	59.72	60.35	
								Inner-wall temperature, T <sub>w</sub> , K															
4	10.5	403	293.2	323.7	115	----	----	377.0	397.0	399.0	400.0	400.0	400.0	400.0	399.0	401.0	400.0	397.0	393.0	389.0	394.0	391.5	
5	10.5	545	292.6	334.3	115	----	----	( <sup>a</sup> )	( <sup>b</sup> )	( <sup>c</sup> )	255.0	403.0	403.0	403.0	403.0	403.0	403.0	403.0	398.0	389.0	395.0	(b)	
8	5.95	530	291.5	333.2	115	----	----	401.5	406.5	414.0	406.0	406.0	406.0	406.0	406.0	406.0	406.0	405.0	398.0	394.0	399.0	398.0	
14	10.5	326	390.9	374.8	153	.040	34	400.0	401.5	401.0	400.0	399.0	399.0	398.0	397.0	396.0	395.0	394.0	394.0	391.5	393.0	390.0	
15	10.5	517	390.9	375.4	154	.053	34	410.0	413.0	413.0	412.0	409.0	406.0	405.0	403.0	401.0	400.0	399.0	398.0	395.0	397.0	395.0	
11	11.3	690	294.3	322.1	117	----	----	381.0	396.0	398.0	400.0	399.0	401.0	400.0	401.0	401.5	403.0	402.0	399.0	393.0	400.0	395.0	
12	12.0	924	294.8	332.1	117	----	----	405.0	411.5	410.0	410.0	409.0	410.0	409.0	405.0	408.0	409.0	408.0	401.0	396.5	404.0	400.0	
13	11.3	1220	295.4	343.7	117	----	----	-----	411.5	411.0	413.0	413.0	413.0	411.0	411.0	411.0	409.0	407.0	403.0	404.0	405.0	401.5	
19	10.4	687	385.9	374.8	153	.061	24	414.0	418.0	416.5	417.0	414.0	413.0	410.0	407.0	405.0	404.0	403.0	403.0	398.0	400.0	398.0	
20	10.0	593	384.3	377.1	170	.078	33	418.0	398.0	423.0	423.0	419.0	418.0	415.0	413.0	412.0	410.0	408.0	411.0	407.0	405.0	405.0	
21	10.0	1252	392.6	379.8	210	.102	55	429.0	430.0	430.0	430.0	428.0	428.0	427.0	426.0	424.0	423.0	421.0	418.0	416.5	418.0	415.0	
22	10.0	1259	385.4	378.7	187	.163	45	421.0	426.0	419.0	426.0	424.0	425.0	426.0	422.0	421.5	420.0	418.0	415.0	414.0	415.0	413.0	
23	10.5	1259	385.9	377.1	173	.201	42	419.0	423.0	422.0	423.0	421.5	422.0	421.5	420.0	419.0	419.0	416.5	414.0	413.0	413.0	410.0	
24	10.0	1343	386.5	377.6	170	.241	41	419.0	422.0	421.0	424.0	422.0	423.0	422.0	421.0	420.0	418.0	416.5	413.0	412.0	413.0	411.0	
25	10.0	1359	385.4	377.1	163	.303	36	416.5	421.5	420.0	421.5	420.0	421.5	420.0	419.0	418.0	415.0	413.0	411.5	412.0	411.0	411.0	
26	10.5	1352	384.3	375.9	154	.377	32	414.0	420.0	418.0	420.0	420.0	420.0	418.0	417.0	415.0	414.0	411.0	410.0	410.0	407.0	407.0	
27	10.4	1362	383.7	374.8	152	.446	30	( <sup>a</sup> )	( <sup>a</sup> )	( <sup>c</sup> )	( <sup>e</sup> )	( <sup>e</sup> )	( <sup>c</sup> )	( <sup>c</sup> )	( <sup>e</sup> )	( <sup>e</sup> )	( <sup>e</sup> )	( <sup>e</sup> )	( <sup>e</sup> )	( <sup>e</sup> )	( <sup>e</sup> )	406.5	
28	10.0	1595	387.6	378.2	239	.149	79	436.0	435.0	435.0	437.0	434.0	435.0	435.0	433.0	433.0	432.0	430.0	426.0	(d)	425.0	424.0	
29	10.0	1589	389.8	377.1	221	.204	77	432.0	435.0	434.0	436.5	434.0	435.0	435.0	433.0	432.0	432.0	430.0	425.0	(d)	425.0	424.0	
30	10.0	1589	388.2	376.5	202	.315	72	431.0	431.0	431.0	434.0	432.0	433.0	434.0	431.5	431.5	427.0	428.0	424.0	421.5	424.0	423.0	
31	10.0	1589	389.8	375.9	195	.360	70	430.0	431.5	430.0	435.0	430.0	430.0	435.0	430.0	430.0	427.0	427.0	424.0	(d)	422.0	421.5	
32	10.0	1592	387.6	375.4	186	.424	64	425.0	428.0	435.0	431.0	430.0	430.0	432.0	430.0	429.0	428.0	425.0	421.5	419.0	420.0	418.0	
33	10.0	1592	388.7	374.8	181	.476	61	424.0	430.0	429.0	430.0	431.0	430.0	431.5	428.0	428.0	426.5	423.0	418.0	418.0	414.0	414.0	

<sup>a</sup>Nonboiling.  
<sup>b</sup>Subcooled boiling.  
<sup>c</sup>Fluctuating.  
<sup>d</sup>Net-quality boiling.  
<sup>e</sup>Automatic shutdown.

TABLE IV. - EXPERIMENTAL DATA FOR 0.584-CENTIMETER INSIDE DIAMETER BY 61-CENTIMETER-LONG TEST SECTION 230-100

[G = mass velocity, kg.(sec)(m<sup>2</sup>); q - heat flux, kW m<sup>-2</sup>; T<sub>1</sub> - inlet temperature, K; T<sub>e</sub> = exit temperature, K; P<sub>e</sub> = exit pressure, kN/m<sup>2</sup> abs; ΔP = pressure drop, kN/m<sup>2</sup>; x<sub>e</sub> = exit quality.]

Run	G	q	T <sub>1</sub>	T <sub>e</sub>	P <sub>e</sub>	ΔP	x <sub>e</sub>	Axial distance from start of heating, z, cm															
								5.080	10.16	15.24	20.32	25.40	30.48	35.56	40.64	45.72	50.80	55.88	57.15	57.15	57.78	57.78	
								Inner-wall temperature, T <sub>w</sub> , K															
67	21.0	1790	294.3	350.4	114	----	----	399.0	392.0	391.0	392.0	395.0	399.0	403.0	403.0	404.0	400.0	400.0	399.0	403.0	400.0	400.0	
68	23.2	2153	294.3	362.6	114	----	----	398.0	403.0	406.0	407.0	408.0	404.0	406.0	403.0	405.0	402.0	401.5	399.0	401.5	400.0	401.5	
71	40.2	1595	293.2	333.2	114	----	----	373.0	378.0	379.0	380.0	380.0	382.0	386.0	388.0	389.0	393.0	391.0	393.0	393.0	393.0	393.0	397.0
72	40.2	3215	294.3	355.4	114	----	----	( <sup>a</sup> )	395.0	400.0	408.0	406.5	409.0	407.0	403.0	405.0	403.0	( <sup>a</sup> )	402.0	401.5	402.0	402.0	
73	40.2	3467	294.8	363.7	114	----	----	400.0	407.0	414.0	415.0	416.0	413.0	414.0	413.0	409.0	411.5	408.0	408.0	405.0	405.0	405.0	
74	40.2	3845	295.4	370.4	114	----	----	413.0	415.0	419.0	420.0	420.0	415.0	415.0	414.0	412.0	414.0	409.0	408.0	408.0	405.0	407.0	
75	40.2	3540	295.4	373.2	114	.0007		414.0	418.0	421.5	423.0	422.0	418.0	419.0	418.0	414.0	417.0	411.5	410.0	408.0	408.0	409.0	

<sup>a</sup>Subcooled boiling.  
<sup>b</sup>Nonboiling.

# ***Error***

---

An error occurred while processing this page. See the system log for more details.

Axial distance from start of heating, z, cm							1.27	3.81	6.35	8.89	11.43	13.97	16.51	19.05	21.59	24.13	26.67	27.30	27.90	28.57
1C	27.4	2673	292.1	334.3	115	13	b406.0	b396.0	b400.0	b408.0	-----	b411.5	b413.0	b413.0	-----	b411.5	b408.0	b406.0	b410.0	b406.0
3C	28.1	2244	310.9	346.5	115	13	b413.0	b414.0	b416.0	b419.0	b418.0	b413.0	b410.0	b412.0	b405.0	b407.0	b406.0	b405.0	b408.0	b404.0
6C	27.8	1992	332.6	365.4	115	24	b413.0	b414.0	b413.0	b413.0	b415.0	b411.5	b413.0	b413.0	-----	b412.0	b407.0	b408.0	b410.0	b404.0
9C	14.3	1504	290.9	339.8	114	9	b405.0	b405.0	b406.0	b408.0	b409.0	b405.0	b408.0	b408.0	b405.0	b406.0	b403.0	b404.0	b411.0	b400.0
10C	14.4	1806	290.9	349.8	114	10	b403.0	b407.0	b409.0	b411.0	b411.0	b407.0	b409.0	b410.0	b408.0	b408.0	b406.0	b404.0	b410.0	b402.0
11C	14.4	2065	290.9	357.6	114	10	b403.0	b407.0	b408.0	b411.0	b410.0	b408.0	b410.0	b411.0	b410.0	b409.0	b405.0	b404.0	b411.0	b404.0
13C	14.1	2058	292.1	359.3	310	8	a431.0	a435.0	a436.0	b438.0	b438.0	b438.0	b440.0	b438.0	b435.0	b438.0	b434.0	b430.0	b434.0	b430.0
14C	14.1	2248	292.1	368.2	310	9	b430.0	b434.0	b434.0	b436.0	b435.0	b436.0	b438.0	b439.0	b435.0	b439.0	b435.0	b431.5	b435.0	b431.5
15C	14.3	2723	292.6	380.9	310	10	b433.0	b437.0	b437.0	b438.0	b438.0	b438.0	b440.0	b439.0	b437.0	b439.0	b436.5	b433.0	b435.0	b433.0
17C	14.1	2251	313.2	388.2	310	14	a431.5	b434.0	b434.0	b435.0	b435.0	b435.0	b436.0	b436.5	b433.0	b436.0	b433.0	b429.0	b433.0	b430.0
19C	14.4	1740	339.8	395.4	310	14	a431.5	b435.0	b434.0	b434.0	b434.0	b433.0	b434.0	b434.0	b433.0	b433.0	b431.5	b428.0	b431.5	b429.0
21C	27.3	3373	337.6	391.5	311	28	a435.0	b438.0	b437.0	b439.0	b439.0	b438.0	b440.0	b442.0	b436.0	b440.0	b436.0	b432.0	b436.0	b434.0
23C	27.0	2679	353.2	395.9	311	26	a435.0	b437.0	b437.0	b439.0	b439.0	b438.0	b439.0	b440.0	b435.0	b438.0	b434.0	b431.0	b436.0	b433.0
25C	28.7	2345	292.1	368.7	447	8	a444.0	a446.5	b448.0	b449.0	b449.0	b450.0	b451.5	b449.0	b449.0	b449.0	b446.5	b444.0	b449.0	b447.0
26C	28.5	2582	292.1	389.3	447	8	a443.0	b446.5	b446.5	b449.0	b448.0	b448.0	b449.0	b449.0	b448.0	b449.0	b446.5	b444.0	b446.5	b445.0
28C	14.4	2607	314.3	396.5	448	12	a441.0	b445.0	b445.0	b448.0	b446.5	b447.0	b448.0	b448.0	b446.0	b448.0	b445.0	b443.0	b445.0	b442.0
30C	70.1	6115	299.3	339.8	117	26/ 30	a400.0	a401.5	a405.0	b415.0	b415.0	b416.0	b419.0	b421.0	b414.0	b419.0	b414.0	b412.0	b413.0	b413.0
37C	70.2	6493	299.8	343.2	117	35/ 46	a399.0	a409.0	a414.0	b418.0	b416.5	b416.5	b419.0	b423.0	b415.0	b421.0	b416.0	b412.0	b414.0	b414.0
38C	70.2	6566	300.4	347.1	117	52/ 70	a408.0	a417.0	a420.0	b423.0	b421.0	b424.0	b424.0	b426.5	b419.0	b424.0	b419.0	b415.0	b416.5	b415.0
40C	70.2	4886	325.4	357.6	117	63/ 66	c419.0	c419.0	c418.0	b420.0	c418.0	b419.0	b421.5	b423.0	b416.5	b418.0	b416.0	b414.0	b414.0	b412.0
41C	70.2	5169	326.5	360.9	117	71/ 74	c417.0	c421.5	c419.0	b422.0	c420.0	b421.0	c423.0	b425.0	b419.0	b422.0	b417.0	b415.0	b415.0	b414.0
42C	70.1	5516	325.9	363.2	117	80/ 83	c419.0	c424.0	c424.0	b425.0	b424.0	b424.0	b425.0	b430.0	b421.5	b426.0	b420.0	b418.0	b418.0	b415.0
43C	70.1	6146	326.5	367.6	117	96/101	b423.0	c430.0	b428.0	b430.0	b429.0	b428.0	b431.0	b433.0	b426.0	b431.0	b423.0	b420.0	b421.0	b418.0
44C	70.4	6209	324.8	366.5	117	92/105	b423.0	b429.0	b428.0	b430.0	b429.0	b429.0	b431.0	b433.0	b426.5	b431.0	b424.0	b421.0	b421.5	b421.0
45C	70.1	6493	324.8	368.7	117	103/108	c427.0	c433.0	b431.5	b434.0	b433.0	b433.0	b434.0	b438.0	b429.0	b434.0	b427.0	b424.0	b425.0	b421.5
47C	47.0	5201	297.6	348.7	115	21/ 35	a417.0	c420.0	c419.0	b420.0	c417.0	b418.0	b419.0	b421.5	b415.0	b420.0	b419.0	b413.0	b415.0	b416.0
49C	47.0	4517	310.9	356.5	115	35/ 49	a418.0	c420.0	c417.0	b420.0	c414.0	b415.0	b416.5	b419.0	b413.0	b416.0	b413.0	b410.0	b410.0	b411.0
51C	47.0	5106	323.2	370.9	115	66/ 77	a422.0	b424.0	b421.5	b423.0	b420.0	b421.5	b423.0	b426.0	b418.0	b423.0	b417.0	b414.0	b414.0	b412.0

<sup>a</sup>Nonboiling.

<sup>b</sup>Subcooled boiling.

# ***Error***

---

An error occurred while processing this page. See the system log for more details.



INSIDE DIAMETER-BY 29.2-CENTIMETER-LONG TEST SECTIONS 230-50, 230-50B, 230-50C, AND 230-50E

$T_e$  = exit temperature, K;  $P_e$  = exit pressure, kN/m<sup>2</sup> abs;  $\Delta P$  = pressure drop, kN/m<sup>2</sup>]

Run	G	q	$T_i$	$T_e$	$P_e$	Inner-wall temperature, $T_w$ , K												
						1.27	3.81	6.35	11.43	15.97	16.51	19.02	21.56	24.13	26.67	29.94	28.57	
Axial distance from start of heating, z, cm																		
4E	28.1	2292	324.8	360.9	687	a428.0	a439.0	a442.0	a447.0	a449.0	b451.0	b445.0	b448.0	b450.0	b449.0	b453.0	b449.0	b450.0
11E	28.0	2320	316.5	360.9	689	a439.0	b453.0	b445.0	b446.0	b448.0	b445.0	b449.0	b450.0	b450.0	b453.0	b455.0	b453.0	b453.0
12E	28.4	3295	310.4	360.9	687	a446.0	b448.0	b443.0	b449.0	b450.0	b450.0	b450.0	b453.0	b455.0	b453.0	b456.5	b456.5	b453.0
17E	28.0	3436	304.3	360.9	687	a449.0	b453.0	b448.0	b454.0	b450.0	b453.0	b453.0	b455.0	b458.0	b455.0	b458.0	b455.0	b456.5
18E	28.0	3782	298.7	360.9	687	a454.0	b456.0	b455.0	b455.0	b458.0	b456.0	b455.0	b459.0	b460.0	b459.0	b462.0	b459.0	b460.0
19E	28.1	1545	352.1	383.2	687	a426.5	a435.0	a440.0	a445.0	a447.0	a448.0	a449.0	a500.0	b452.0	b451.0	b453.0	b451.0	b451.0
11E	28.0	2320	345.9	383.2	687	a435.0	a444.0	a447.0	a450.0	b450.0	b451.0	b453.0	b458.0	b453.0	b455.0	b455.0	b453.0	b453.0
12E	28.0	2613	341.5	383.2	687	a446.5	a453.0	a453.0	b455.0	b454.0	b454.0	b456.0	b456.5	b455.0	b458.0	b455.0	b455.0	b455.0
13E	28.0	3152	332.1	383.2	687	a456.5	b458.0	b458.0	b460.0	b460.0	b459.0	b458.0	b459.0	b460.0	b457.0	b460.0	b460.0	b457.0
14E	28.0	3499	325.9	383.2	687	a457.0	b459.0	b460.0	b461.0	b462.0	b460.0	b459.0	b460.0	b461.5	b458.0	b461.0	b459.0	b459.0
16E	28.0	1582	369.3	394.3	688	a426.5	a435.0	a437.0	a443.0	a444.0	a445.0	a446.0	a448.0	b450.0	b449.0	b451.5	b450.0	b450.0
19E	28.0	2665	360.9	394.3	688	a439.0	a450.0	a453.0	a454.0	b455.0	b454.0	b455.0	b455.0	b453.0	b455.0	b455.0	b453.0	b453.0
20E	28.0	2355	355.9	394.3	688	a446.5	b455.0	b454.0	b455.0	b458.0	b456.0	b455.0	b456.0	b458.0	b455.0	b456.0	b456.0	b456.0
21E	28.0	2636	362.1	394.8	689	a441.5	b450.0	a452.0	b457.0	b457.0	b456.0	b455.0	b455.0	b456.5	b455.0	b456.5	b455.0	b455.0
22E	28.0	2780	350.4	394.3	687	a458.0	b458.0	b459.0	b461.0	b461.5	b460.0	b459.0	b461.0	b461.0	b458.0	b452.0	b450.0	b459.0
23E	28.0	3152	343.7	394.3	687	a456.0	b458.0	b460.0	b461.0	b462.0	b460.0	b458.0	b460.0	b462.0	b460.0	b452.0	b452.0	b461.3
24E	28.0	3373	339.8	394.3	688	a457.0	b460.0	b461.0	b461.5	b462.0	b460.0	b459.0	b461.0	b463.0	b463.0	b463.0	b463.0	b462.0
25E	28.1	1532	370.4	394.3	688	a428.0	a434.0	a437.0	a443.0	a445.0	a445.0	a448.0	b450.0	b449.0	b451.0	b451.0	b450.0	b450.0
26E	28.0	1612	389.8	405.4	687	a424.0	a428.0	a430.0	a434.0	a436.0	a435.0	a436.0	a440.0	a441.0	a441.0	a444.0	a444.0	a441.0
27E	28.0	1330	384.3	405.4	687	a433.0	a439.0	a441.5	a446.0	a448.0	a448.0	a448.0	a450.0	b452.0	b450.0	b452.0	b451.5	b451.5
30E	28.0	1879	374.8	405.4	688	a443.0	b451.5	b451.5	b453.0	b454.0	b453.0	b452.0	b454.0	b456.0	b455.0	b454.0	b454.0	b454.0
31E	28.0	2342	368.2	405.4	688	a454.0	b453.0	b454.0	b455.0	b455.0	b454.0	b454.0	b455.0	b457.0	b455.0	b456.5	b454.0	b454.0
32E	28.0	2739	361.5	405.4	688	a450.0	b454.0	b455.0	b457.0	b458.0	b455.0	b458.0	b458.0	b457.0	b457.0	b459.0	b458.0	b458.0
33E	28.0	3295	355.9	405.4	688	a454.0	b458.0	b459.0	b461.0	b461.5	b460.0	b460.0	b461.0	b463.0	b459.0	b452.0	b452.0	b460.0
34E	47.0	2196	333.7	360.9	687	a413.0	a421.0	a424.0	a429.0	a431.5	a432.0	a433.0	a438.0	b441.0	b439.0	b444.0	b444.0	b443.0
35E	47.0	3593	324.8	360.9	687	a429.0	a436.0	a440.0	a447.0	a448.0	a449.0	a450.0	a453.0	b458.0	b454.0	b459.0	b459.0	b456.0
40E	47.0	4224	318.7	360.9	687	a445.0	a454.0	a456.5	b458.0	b460.0	b457.0	b456.0	b460.0	b463.0	b460.0	b454.0	b454.0	b450.0
41E	47.0	4854	312.6	361.2	688	a457.0	a459.0	b460.0	b460.0	b463.0	b460.0	b460.0	b461.5	b464.0	b461.0	b455.0	b463.0	b463.0
42E	47.0	5453	306.5	360.9	689	a461.0	b463.0	b463.0	b463.0	b464.0	b461.5	b460.0	b464.0	b466.5	b463.0	b470.0	b459.0	b459.0
43E	47.0	2449	359.3	383.2	683	a420.0	a425.0	a428.0	a435.0	a436.0	b438.0	b439.0	b443.0	b447.0	b446.0	b451.0	b446.5	b446.5
44E	47.0	2882	354.8	383.2	686	a429.0	a435.0	a440.0	a445.0	a446.5	b450.0	b450.0	a453.0	b456.5	b455.0	b458.0	b458.0	b458.0
46E	47.0	3404	349.8	383.2	687	a439.0	a446.0	a450.0	a456.0	b458.0	b456.5	b456.5	b459.0	b462.0	b458.0	b452.0	b458.0	b458.0
47E	47.0	4003	343.2	383.2	687	a448.0	a456.5	a459.0	b460.0	b461.0	b459.0	b459.0	b461.0	b464.0	b461.0	b454.0	b461.0	b461.0
48E	47.0	4602	337.1	383.2	687	a459.0	-----	-----	b465.0	b466.5	b464.0	b463.0	b465.0	b466.5	b463.0	b456.0	b462.0	b462.0
49E	47.0	5127	329.3	383.2	687	a466.5	b469.0	b469.0	b469.0	b470.0	b468.0	b467.0	b469.0	b473.0	b467.0	b470.0	b465.0	b465.0
50E	47.0	2244	369.9	383.2	687	a420.0	a425.0	a428.0	a431.0	a438.5	b437.0	b437.0	b441.0	b443.0	b444.0	b448.0	b448.0	b449.0
51E	47.0	2020	374.8	394.3	683	a424.0	a429.0	a428.0	a438.0	a440.0	a440.0	a440.0	a444.0	b447.0	b447.0	b449.0	b447.0	b447.0
52E	47.0	2559	368.7	394.3	687	a431.5	a446.0	a448.0	a450.0	a452.0	a453.0	a452.0	a455.0	b458.0	b456.5	b459.0	b458.0	b458.0
53E	47.0	3467	360.4	394.3	687	a446.0	a455.0	a455.0	b458.0	b459.0	b457.0	b456.5	b459.0	b461.5	b459.0	b451.5	b458.0	b458.0
54E	47.0	4066	354.3	394.3	687	a456.5	b463.0	b464.0	b465.0	b466.0	b464.0	b463.0	b464.0	b465.0	b461.5	b461.0	b461.0	b461.0
56E	46.7	4350	350.9	394.3	687	a461.0	b464.0	b465.0	b467.0	b468.0	b465.0	b463.0	b466.0	b468.0	b463.0	b456.0	b462.0	b462.0
57E	46.7	4760	347.1	394.3	687	a465.0	b468.0	b468.0	b469.0	b469.0	b468.0	b466.0	b468.0	b470.0	b464.0	b467.0	b465.0	b465.0
58E	47.0	5012	344.8	394.3	687	a465.0	b468.0	b469.0	b469.0	b469.0	b467.0	b465.0	b468.0	b469.0	b465.0	b469.0	b465.0	b465.0
59E	47.0	5295	342.1	394.3	687	a465.0	b467.0	b469.0	b469.0	b469.0	b466.0	b465.0	b467.0	b470.0	b465.0	b469.0	b465.0	b465.0
60E	47.0	5548	339.6	394.3	687	a465.0	b466.0	b467.0	b466.5	b468.0	b466.0	b464.0	b466.5	b470.0	b465.0	b470.0	b466.5	b466.5
61E	46.7	2155	382.6	405.4	689	a438.0	a444.0	a448.0	a453.0	b454.0	b454.0	b453.0	b458.0	b458.0	b458.0	b450.0	b458.0	b458.0
62E	46.7	3215	373.7	405.4	687	a450.0	a458.0	a461.0	b463.0	b463.0	b461.0	b461.0	b461.5	b463.0	b458.0	b450.0	b458.0	b458.0
63E	46.7	4035	364.8	405.4	685	a458.0	b460.0	b461.0	b463.0	b463.0	b461.5	b460.0	b463.0	b464.0	b461.0	b454.0	b461.5	b461.5
64E	46.7	4413	361.5	405.4	686	a459.0	b460.0	b462.0	b462.0	b463.0	b461.5	b460.0	b462.0	b464.0	b460.0	b454.0	b454.0	b454.0
65E	47.0	5012	355.9	405.4	686	a462.0	b464.0	b465.0	b465.0	b466.0	b464.0	b461.5	b464.0	b466.5	b463.0	b457.0	b454.0	b454.0
66E	47.0	5516	350.9	405.4	686	a464.0	b466.5	b466.5	b466.5	b467.0	b464.0	b463.0	b465.0	b469.0	b463.0	b463.0	b465.0	b465.0
67E	47.0	3651	375.9	405.7	687	a449.0	a458.0	a458.0	a460.0	b461.5	b460.0	b458.0	b460.0	b461.0	b458.0	b450.0	b457.0	b457.0
71E	47.5	1154	405.9	416.5	688	a431.5	a436.0	a437.0	a440.0	a441.5	a441.5	a441.5	a443.0	b445.0	b445.0	b448.0	b446.0	b446.0
72E	47.0	1961	398.2	416.5	689	a444.0	a444.0	a451.5	a455.0	b458.0	b457.0	b456.0	b459.0	b460.0	b460.0	b461.5	b450.0	b460.0
73E	46.7	2289	393.7	416.5	687	a450.0	a456.5	a458.0	b461.0	b461.0	b459.0	b459.0	b461.5	b464.0	b461.0	b450.0	b456.5	b456.5
74E	47.0	2572	387.1	416.5	687	a458.0	a459.0	b460.0	b460.0	b462.0	b461.0	b460.0	b463.0	b464.0	b458.0	b451.5	b458.0	b458.0
75E	47.0	3072	377.6	416.8	687	a462.0	b463.0	b464.0	b464.0	b464.0	b461.5	b460.0</						

TABLE VI. - HEAT-TRANSFER AND PRESSURE DROP DATA FOR 0.584-CENTIMETER INSIDE DIAMETER BY 14.6-CENTIMETER-LONG TEST SECTION 230-25F

[G = mass velocity, kg/(sec)(m<sup>2</sup>); q = heat flux, kW/m<sup>2</sup>; T<sub>i</sub> = inlet temperature, K; T<sub>e</sub> = exit temperature, K; P<sub>e</sub> = exit pressure, kN/m<sup>2</sup> abs; ΔP = pressure drop, kN/m<sup>2</sup>.]

Run	G	q	T <sub>i</sub>	T <sub>e</sub>	P <sub>e</sub>	ΔP	Axial distance from start of heating, z, cm																				
							0.635	1.27	1.88	2.54	3.17	3.81	4.44	5.71	6.98	8.25	9.52	10.79	12.06	12.70	13.33	13.97	14.10	14.29			
							Inner-wall temperature, T <sub>w</sub> , K																				
4	3.54	113	351.2	356.5	114	<7	a370.0	a378.0	a381.0	a385.0	a386.0	a387.0	a388.0	a389.0	a390.0	a391.5	a393.0	b394.0	b389.0	b390.0	b391.5	b391.0	b391.5	b391.0	b393.0	b394.0	
5	3.54	501	342.1	368.2	114	<7	b400.0	b397.0	b399.0	b395.0	b402.0	b402.0	b401.0	b402.0	b399.0	b398.0	b432.0	b402.0	b395.0	b398.0	b398.0	b398.0	b398.0	b398.0	b398.0	b400.0	b400.0
6	3.52	602	296.5	335.9	114	~7	b402.0	b398.0	b399.0	b398.0	b403.0	b407.0	b403.0	b405.0	b402.0	b403.0	b432.0	b399.0	b403.0	b404.0	b403.0	b403.0	b403.0	b403.0	b405.0	b403.0	
10	7.01	646	293.2	314.3	114	<7	a389.0	b399.0	b398.0	b397.0	b401.0	b401.5	b401.5	b404.0	b404.0	b403.0	b405.0	-----	-----	b403.0	-----	b398.0	b404.0	b403.0	b403.0	b403.0	
12	7.01	224	350.9	314.3	114	<7	a375.0	a380.0	a383.0	a384.0	a385.0	a386.5	a388.0	a389.0	a390.0	a390.0	a390.0	a390.0	a390.0	a391.5	a391.5	a390.0	a392.0	a392.0	a392.0	a393.0	a393.0
13	7.05	372	351.5	314.3	114	<7	b391.5	b397.0	b397.0	b395.0	b401.0	b396.5	b401.0	b402.0	b396.0	b401.0	b401.5	b401.5	b395.0	b395.0	b396.0	b396.0	b396.0	b396.0	b396.0	b396.0	b399.0
14	7.01	589	347.3	314.3	114	<7	b399.0	b399.0	b400.0	b397.0	b404.0	b405.0	b403.0	b404.0	b401.0	b401.0	b404.0	b401.5	b398.0	b399.0	b399.0	b399.0	b399.0	b399.0	b399.0	b403.0	b401.0
28	7.02	649	375.9	394.3	687	10	a433.0	a443.0	a445.0	b445.0	b445.0	b446.0	b446.0	b447.0	b448.0	b448.0	b449.0	b449.0	b449.0	b449.0	b449.0	b448.0	b451.5	b446.5	b452.0	b451.5	b451.5
161	28.1	3215	293.2	319.6	112	13	b414.0	b414.0	b414.0	b415.0	b420.0	b420.0	b416.5	b421.0	b425.0	b420.0	b421.0	b421.0	b421.0	b421.0	b421.0	b420.0	b425.0	b417.0	b424.0	b422.0	b422.0
162	28.1	3215	298.2	324.3	112	12	b415.0	b414.0	b415.0	b416.5	b421.0	b420.0	b419.0	b421.0	b425.0	b419.0	b418.0	b420.0	b419.0	b419.0	b419.0	b419.0	b425.0	b416.5	b423.0	b422.0	b422.0
163	28.0	3215	303.5	327.6	112	12	b414.0	b414.0	b415.0	b416.5	b420.0	b420.0	b420.0	b421.0	b425.0	b418.0	b418.0	b419.0	b419.0	b419.0	b419.0	b425.0	b416.5	b423.0	b422.0	b422.0	
164	28.0	3184	303.4	329.8	112	13	b414.0	b413.0	b415.0	b416.0	b420.0	b419.0	b418.0	b419.0	b421.0	b418.0	b419.0	b419.0	b419.0	b419.0	b419.0	b424.0	b415.0	b421.5	b420.0	b420.0	
165	28.1	3184	307.1	333.4	112	14	b413.0	b412.0	b414.0	b416.0	b419.0	b418.0	b419.0	b419.0	b421.0	b418.0	b421.0	b421.0	b421.0	b421.0	b421.0	b425.0	b416.5	b422.0	b421.0	b421.0	
166	28.0	3184	310.9	337.1	112	13	b415.0	b413.0	b416.5	b416.5	b420.0	b419.0	b420.0	b421.5	b418.0	b418.0	b419.0	b419.0	b419.0	b419.0	b419.0	b424.0	b416.0	b421.5	b421.0	b421.0	
167	28.1	3184	313.2	339.3	112	14	b414.0	b413.0	b415.0	b416.5	b420.0	b419.0	b418.0	b420.0	b421.5	b418.0	b420.0	b418.0	b419.0	b419.0	b419.0	b422.0	b415.0	b420.0	b420.0	b420.0	
168	28.1	3184	315.1	340.9	112	14	b415.0	b414.0	b416.5	b416.5	b421.5	b420.0	b419.0	b420.0	b421.5	b419.0	b420.0	b419.0	b419.0	b418.0	b418.0	b423.0	b415.0	b421.0	b420.0	b420.0	
169	28.1	3184	318.7	344.3	112	14	b415.0	b414.0	b416.5	b417.0	b421.0	b420.0	b419.0	b420.0	b421.5	b418.0	b420.0	b419.0	b418.0	b418.0	b418.0	b421.5	b414.0	b419.0	b420.0	b420.0	
170	28.0	3184	320.9	346.8	112	13/14	b416.5	b415.0	b417.0	b418.0	b421.5	b420.0	b419.0	b419.0	b420.0	b415.5	b417.0	b419.0	b418.0	b418.0	b416.5	b422.0	b414.0	b421.0	b420.0	b420.0	
227	28.0	3184	297.1	323.4	308	12	b436.0	b437.0	b439.0	b439.0	b441.0	b441.0	b441.5	b442.0	b444.0	b444.0	b444.0	b444.0	b444.0	b444.0	b444.0	b445.0	b446.5	b451.0	b443.0	b447.0	b446.0
228	28.0	3184	301.2	327.6	308	12	b436.0	b436.0	b438.0	b439.0	b440.0	b440.0	b441.0	b441.5	b444.0	b444.0	b444.0	b444.0	b444.0	b444.0	b444.0	b445.0	b446.0	b450.0	b443.0	b446.5	b446.5
229	28.0	3184	304.8	330.7	308	13	b436.0	b436.0	b439.0	b439.0	b440.0	b440.0	b441.0	b441.5	b444.0	b444.0	b444.0	b444.0	b444.0	b444.0	b444.0	b445.0	b446.0	b450.0	b443.0	b446.5	b446.5
230	28.0	3215	307.6	333.7	308	14	b436.0	b438.0	b439.0	b439.0	b441.0	b441.0	b441.5	b441.5	b444.0	b444.0	b444.0	b444.0	b444.0	b444.0	b444.0	b445.0	b446.5	b451.0	b443.0	b447.0	b447.0
231	28.0	3184	311.5	337.6	308	14	b438.0	b438.0	b440.0	b440.0	b442.0	b441.5	b442.0	b443.0	b445.0	b444.0	b444.0	b444.0	b444.0	b444.0	b444.0	b445.0	b446.0	b450.0	b444.0	b447.0	b447.0
232	28.0	3215	315.4	341.8	308	14	b437.0	b438.0	b440.0	b440.0	b442.0	b441.5	b442.0	b443.0	b445.0	b444.0	b444.0	b444.0	b444.0	b444.0	b444.0	b445.0	b446.5	b450.0	b444.0	b446.5	b446.5
233	28.0	3215	320.9	347.1	308	14	b439.0	b438.0	b441.0	b441.0	b443.0	b443.0	b443.0	b443.0	b446.0	b445.0	b444.0	b444.0	b444.0	b444.0	b444.0	b445.0	b446.0	b450.0	b444.0	b446.5	b446.5
234	28.0	3215	323.7	349.8	308	14	b440.0	b440.0	b442.0	b442.0	b443.0	b443.0	b443.0	b443.0	b446.0	b445.0	b444.0	b444.0	b444.0	b444.0	b444.0	b445.0	b446.5	b450.0	b444.0	b447.0	b447.0
235	28.0	3215	327.1	353.2	308	14	b439.0	b439.0	b441.5	b443.0	b444.0	b444.0	b444.0	b444.0	b446.5	b445.0	b444.0	b444.0	b444.0	b444.0	b444.0	b445.0	b446.5	b450.0	b444.0	b446.5	b446.5
236	28.0	3215	331.2	357.3	308	14	b440.0	b439.0	b443.0	b443.0	b444.0	b444.0	b444.0	b444.0	b446.5	b446.0	b446.0	b446.0	b446.0	b446.0	b446.0	b445.0	b446.5	b450.0	b444.0	b447.0	b447.0
237	28.0	3247	335.1	361.2	308	14	b443.0	b441.5	b444.0	b444.0	b445.0	b445.0	b445.0	b445.0	b447.0	b446.0	b446.0	b446.0	b446.0	b446.0	b446.0	b445.0	b446.5	b450.0	b444.0	b446.5	b446.5
238	28.0	3247	338.2	364.3	308	14	b443.0	b443.0	b445.0	b445.0	b446.5	b446.5	b446.5	b446.5	b448.0	b447.0	b447.0	b447.0	b447.0	b447.0	b447.0	b446.5	b450.0	b444.0	b446.5	b446.5	
239	28.0	3247	339.6	365.7	308	14	b443.0	b441.5	b444.0	b445.0	b446.5	b446.5	b446.5	b446.5	b448.0	b447.0	b447.0	b447.0	b447.0	b447.0	b447.0	b446.5	b450.0	b444.0	b446.5	b446.5	
240	28.0	3247	340.9	366.8	308	14/15	b444.0	b443.0	b445.0	b446.0	b446.5	b446.5	b446.5	b446.5	b448.0	b447.0	b447.0	b447.0	b447.0	b447.0	b447.0	b446.5	b450.0	b444.0	b446.5	b446.5	
241	28.0	3278	343.7	366.8	308	14/15	b443.0	b443.0	b445.0	b445.0	b446.5	b446.5	b446.5	b446.5	b448.0	b447.0	b447.0	b447.0	b447.0	b447.0	b447.0	b446.5	b450.0	b444.0	b446.5	b446.5	
242	28.0	3247	347.1	373.2	309	14/16	b443.0	b443.0	b445.0	b446.0	b446.5	b446.5	b446.5	b446.5	b448.0	b447.0	b447.0	b447.0	b447.0	b447.0	b447.0	b446.5	b450.0	b444.0	b446.5	b446.5	
243	27.7	3215	349.6	375.4	309	14/16	b441.5	b441.0	b444.0	b444.0	b445.0	b445.0	b445.0	b445.0	b447.0	b446.0	b446.0	b446.0	b446.0	b446.0	b446.0	b445.0	b446.5	b450.0	b444.0	b446.5	
244	28.0	3184	354.6	380.4	308	14/17	b442.0	b441.0	b444.0	b442.0	b444.0	b443.0	b444.0	b444.0	b446.0	b445.0	b445.0	b445.0	b445.0	b445.0	b445.0	b445.0	b446.0	b448.0	b442.0	b446.0	b445.0
245	27.7	3215	357.3	382.9	308	14/19	b443.0	b441.5	b445.0	b445.0	b446.5	b446.5	b446.5	b446.5	b448.0	b447.0	b447.0	b447.0	b447.0	b447.0	b447.0	b446.5	b450.0	b444.0	b446.5	b446.5	
246	28.0	3215	361.8	387.6	308	16/23	b444.0	b443.0	b444.0	b443.0	b444.0	b444.0	b444.0	b444.0	b446.5	b445.0	b445.0	b445.0	b445.0	b445.0	b445.0	b445.0	b446.0	b448.0	b441.5	b445.0	b444.0
247	28.0	3215	364.8	390.4	308	17/26	b443.0	b441.5	b444.0	b443.0	b444.0	b444.0	b444.0	b444.0	b446.5	b445.0	b445.0	b445.0	b445.0	b445.0	b445.0	b445.0	b446.5	b448.0	b441.5	b445.0	b444.0
248	27																										



TABLE VII. - HEAT-TRANSFER AND PRESSURE DROP DATA FOR 0.584-CENTIMETER INSIDE DIAMETER BY 14.6-CENTIMETER-LONG TEST SECTIONS 230-25,

230-25B, 230-25C, AND 230-25D

[G = mass velocity, kg/(sec)(m<sup>2</sup>); q = heat flux, kW/m<sup>2</sup>; T<sub>i</sub> = inlet temperature, K; T<sub>e</sub> = exit temperature, K; P<sub>e</sub> = exit pressure, kN/m<sup>2</sup> abs; ΔP = pressure drop, kN/m<sup>2</sup>.]

Run	G	q	T <sub>i</sub>	T <sub>e</sub>	P <sub>e</sub>	ΔP	Inner-wall temperature, T <sub>w</sub> , K													
							Axial distance from start of heating, z, cm													
							0.635	1.94	3.17	4.44	5.71	6.98	8.25	9.52	10.79	12.06	12.70	13.30	14.04	13.97
3	28.1	2106	293.2	310.9	115	<7	a390.0	b415.0	b415.0	-----	b403.0	b408.0	b409.0	b409.0	b410.0	b411.0	b439.0	b409.0	b408.0	b408.0
4	28.1	2783	293.2	316.5	115	<7	a416.5	b431.5	b431.5	-----	b414.0	b416.5	b418.0	b416.5	b418.0	b418.0	b416.5	b416.0	b414.0	b415.0
5	28.4	4129	293.7	327.6	115	<7	b419.0	b435.0	b418.0	-----	b416.0	b415.0	b419.0	b414.0	b419.0	b416.5	b414.0	b412.0	b413.0	b415.0
6	28.1	4570	293.7	331.5	115	7	b420.0	b419.0	b418.0	-----	b418.0	b419.0	b419.0	b415.0	b418.0	b418.0	b413.0	b413.0	b413.0	b415.0
7	28.7	4823	293.7	333.7	115	7	b422.0	b420.0	b419.0	-----	b418.0	b420.0	b421.5	b416.0	b420.0	b419.0	b415.0	b414.0	b416.0	b418.0
8	28.1	4949	294.3	334.8	115	7	b423.0	b421.0	b420.0	-----	b419.0	b421.0	b423.0	b416.0	b420.0	b419.0	b417.0	b416.0	b418.0	b419.0
9	28.1	5043	294.3	335.9	115	8	b424.0	b420.0	b420.0	-----	b420.0	b421.0	b423.0	b419.0	b421.0	b420.0	b418.0	b417.0	b418.0	b420.0
10	28.1	5201	294.3	337.1	115	8	b422.0	b421.0	b421.0	-----	b420.0	b421.5	b423.0	b420.0	b421.5	b420.0	b418.0	b419.0	b419.0	b421.0
11	28.4	3845	313.2	344.3	115	6	b427.0	b424.0	b421.0	-----	b419.0	b417.0	b420.0	b416.5	b418.0	b416.0	b414.0	b415.0	b415.0	b416.0
12	28.1	4066	312.6	345.9	115	8	b425.0	b422.0	b420.0	-----	b419.0	b419.0	b420.0	b417.0	b419.0	b417.0	b416.0	b417.0	b416.5	b418.0
13	28.4	4224	313.2	347.6	115	11	b426.0	b424.0	b423.0	-----	b420.0	b420.0	b422.0	b417.0	b419.0	b420.0	b419.0	b419.0	b418.0	b419.0
14	28.1	4413	313.2	348.7	115	13	b426.0	b424.0	b422.0	-----	b421.0	b419.0	b422.0	b418.0	b420.0	b420.0	b419.0	b419.0	b420.0	b420.0
15	28.1	4602	313.2	350.9	115	15	b425.0	b425.0	b424.0	-----	b421.0	b420.0	b422.0	b419.0	b421.5	b423.0	b420.0	b420.0	b420.0	b422.0
16	28.1	4823	313.2	352.6	115	19	b426.0	b426.0	b424.0	-----	b420.0	b420.0	b423.0	b421.0	b423.0	b423.0	b420.0	b420.0	b420.0	b421.5
18	27.8	2818	331.5	355.4	115	12	b417.0	b413.0	b413.0	-----	b406.5	b407.0	b408.0	b402.0	b405.0	b405.0	b403.0	b403.0	b400.0	b403.0
19	27.8	3184	331.5	358.7	115	16	b429.0	b425.0	b419.0	-----	b420.0	b421.0	b423.0	b419.0	b421.0	b420.0	b416.5	b419.0	b416.0	b419.0
20	28.4	3530	330.9	360.7	115	20	b428.0	b426.5	b420.0	-----	b419.0	b419.0	b423.0	b418.0	b421.5	b420.0	b415.0	b417.0	b415.0	b417.0
21	27.6	3940	331.5	363.7	115	26	b429.0	b428.0	b423.0	-----	b420.0	b422.0	b424.0	b421.0	b421.0	b421.0	b421.5	b417.0	b416.0	b418.0
22	28.1	4224	330.9	364.8	115	30	b429.0	b428.0	b422.0	-----	b420.0	b423.0	b425.0	b420.0	b421.5	b422.0	b418.0	b418.0	b416.5	b419.0
23	28.1	4602	330.9	368.2	115	36	b433.0	b428.0	b426.5	-----	b425.0	b427.0	b428.0	b424.0	b424.0	b426.5	b421.5	b421.5	b419.0	b421.5
							0.61	1.90	3.17	4.44	5.71	6.98	8.25	9.52	10.79	12.11	12.70	13.33	13.39	13.97
28	28.7	3593	293.7	322.1	114	10	b414.0	b411.0	b412.0	b414.0	b415.0	b415.0	b414.0	b414.0	b414.0	b408.0	b439.0	b408.0	b412.0	b410.0
48	45.9	4066	294.3	315.4	115	12	b404.0	b400.0	b402.0	b400.0	b401.5	b402.0	b400.0	b401.0	b401.0	b399.0	b430.0	b401.5	b401.5	b403.0
58	45.9	6367	295.4	328.2	115	16	b425.0	b424.0	b425.0	b424.0	b425.0	b425.0	b420.0	b423.0	b420.0	b416.5	b419.0	b421.5	b420.0	b421.0
68	45.9	6714	295.9	329.8	115	17	b425.0	b425.0	b426.0	b425.0	b426.0	b426.5	b423.0	b424.0	b421.0	b418.0	b421.0	b424.0	b422.0	b423.0
88	45.9	6146	304.3	334.8	115	17	b425.0	b425.0	b426.0	b424.0	b425.0	b425.0	b423.0	b423.0	b420.0	b418.0	b420.0	b423.0	b419.0	b423.0
108	45.6	3814	323.7	343.2	115	14	b425.0	b422.0	b421.5	b418.0	b416.5	b414.0	b414.0	b414.0	b412.0	b410.0	b412.0	b414.0	b414.0	b415.0
118	45.9	4570	323.7	346.5	115	19	b422.0	b420.0	b421.0	b418.0	b416.0	b416.5	b415.0	b416.0	b414.0	b411.0	b413.0	b415.0	b416.0	b418.0
128	45.9	4066	330.4	350.9	115	23	b426.5	b424.0	b426.0	b424.0	b421.5	b421.5	b420.0	b418.0	b415.0	b418.0	b419.0	b411.0	b411.0	b414.0
148	45.9	4507	324.3	346.5	115	19	b423.0	b420.0	b422.0	b420.0	b418.0	b417.0	b416.0	b417.0	b414.0	b412.0	b414.0	b416.5	b415.0	b415.0
168	28.2	4696	294.3	333.2	310	10	b447.0	b448.0	b448.0	b448.0	b449.0	b449.0	b448.0	b448.0	b448.0	b445.0	b447.0	b449.0	b446.5	b450.0
178	28.4	5138	294.3	337.1	308	10	b444.0	b445.0	b446.0	b446.0	b446.0	b446.5	b444.0	b446.0	b445.0	b441.5	b444.0	b445.0	b448.0	b447.0
188	28.2	5737	294.8	341.5	306	11	b446.5	b446.0	b448.0	b446.0	b446.5	b446.5	b444.0	b445.0	b444.0	b443.0	b444.0	b446.0	b449.0	b449.0
198	28.2	5989	294.8	343.7	308	12	b448.0	b448.0	b448.0	b448.0	b448.0	b448.0	b446.5	b448.0	b446.5	b445.0	b445.0	b447.0	b449.0	b449.0
208	28.2	6462	294.8	347.6	308	10/14	b448.0	b448.0	b447.0	b446.0	b447.0	b447.0	b445.0	b446.5	b445.0	b444.0	b444.0	b446.0	b448.0	b448.0
218	28.2	6503	294.8	352.1	308	10/16	b448.0	b448.0	b448.0	b448.0	b448.0	b448.0	b446.0	b447.0	b446.0	b445.0	b445.0	b447.0	b449.0	b448.0
228	28.4	6934	294.8	354.3	308	10/18	b449.0	b449.0	b449.0	b447.0	b449.0	b449.0	b446.0	b448.0	b446.0	b445.0	b446.0	b447.0	b450.0	b449.0
248	28.7	4444	310.9	344.3	310	10	b441.5	b441.0	b439.0	b438.0	b439.0	b439.0	b436.5	b438.0	b436.0	b435.0	b435.0	b436.5	b437.0	b438.0
258	28.4	6430	310.9	362.6	310	10/17	b448.0	b446.5	b448.0	b445.0	b448.0	b448.0	b444.0	b446.0	b444.0	b443.0	b444.0	b445.0	b446.5	b446.5
268	28.2	6682	310.9	364.8	310	0/21	b446.0	b446.0	b447.0	b445.0	b446.0	b444.0	b445.0	b444.0	b442.0	b443.0	b443.0	b443.0	b445.0	b445.0
288	28.2	3247	332.1	357.6	309	10	b430.0	b428.0	b428.0	b428.0	b429.0	b428.0	b427.0	b428.0	b427.0	b425.0	b428.0	b429.0	b431.0	b430.0
298	28.4	4633	331.5	370.4	309	11/15	b445.0	b443.0	b444.0	b443.0	b444.0	b444.0	b442.0	b443.0	b441.0	b440.0	b441.0	b441.5	b443.0	b442.0

31B	28.4	3972	353.7	385.4	310	6/22	b436.5	b436.5	b436.5	b436.0	b437.0	b436.5	b435.0	b435.0	b434.0	b433.0	b434.0	b435.0	b436.5	b436.0
32B	28.2	4287	352.6	387.1	310	3/31	b439.0	b439.0	b439.0	b438.0	b439.0	b439.0	b436.5	b437.0	b435.0	b435.0	b436.0	b437.0	b437.0	b439.0
33B	46.0	5264	319.3	345.4	115	22	a421.0	b436.0	b436.0	b433.0	b435.0	b434.0	b433.0	b434.0	b433.0	b433.0	b423.0	b423.0	b418.0	b418.0
34B	45.9	6745	319.6	353.2	115	41/55	b426.5	b424.0	b425.0	b423.0	b425.0	b424.0	b423.0	b424.0	b422.0	b422.0	b422.0	b421.0	b422.0	b421.0
35B	45.9	6966	317.6	352.6	115	41/55	b428.0	b424.0	b426.5	b424.0	b426.5	b426.5	b424.0	b424.0	b423.0	b423.0	b423.0	b423.0	b423.0	b423.0
37B	14.3	1768	294.8	322.6	114	8	b416.0	b404.0	b404.0	b406.5	b406.5	b406.5	b406.5	b407.0	-----	-----	-----	-----	b404.0	-----
38B	14.4	3341	294.3	347.1	114	10	b404.0	b406.0	b408.0	b409.0	b409.0	b410.0	b408.0	b408.0	b407.0	b406.5	b408.0	b408.0	b410.0	b409.0
39B	45.9	5453	312.1	338.7	115	17	b423.0	b416.0	b417.0	b415.0	b415.0	b414.0	b414.0	b415.0	b413.0	b414.0	b414.0	b414.0	b416.0	b415.0
Axial distance from start of heating, z, cm							0.635	1.90	3.14	4.44	5.71	6.96	8.25	9.52	10.82	12.06	12.70	13.28	14.00	14.00
3C	28.7	4917	294.3	334.8	114	6	b409.0	b408.0	b409.0	b411.0	b409.0	b411.0	-----	b410.0	b406.0	b409.0	b409.0	b409.0	b411.5	b411.0
4C	28.7	4570	305.4	341.5	115	8	b415.0	b411.0	b411.0	b414.0	b408.0	b411.0	-----	b411.0	b406.5	b409.0	b410.0	b412.0	b419.0	b412.0
5C	28.1	3940	314.3	345.9	115	8	b419.0	b412.0	b411.5	b412.0	b407.0	b409.0	-----	b410.0	b406.0	b409.0	b409.0	b411.5	b417.0	b411.5
6C	28.4	3688	323.2	350.9	115	8	b420.0	b410.0	b411.0	b410.0	b406.5	b406.5	-----	b408.0	b405.0	b406.5	b409.0	b409.0	b415.0	b409.0
7C	28.1	2957	332.1	355.4	115	8	b425.0	b411.0	b408.0	b410.0	b406.0	b408.0	-----	b410.0	b407.0	b409.0	b409.0	b413.0	b415.0	b409.0
8C	28.1	3404	348.7	373.7	114	37/41	b416.5	b415.0	b412.0	b414.0	b412.0	b415.0	-----	b415.0	b411.0	b413.0	b412.0	b414.0	b418.0	b411.5
25C	105.0	10276	302.6	324.8	119	28/34	b413.0	b410.0	b408.0	b412.0	b409.0	b414.0	-----	b409.0	b407.0	b409.0	b408.0	b410.0	b408.0	b407.0
26C	105.0	8573	313.2	332.6	119	28/36	b416.0	b413.0	b412.0	b416.0	b413.0	b417.0	-----	b413.0	b415.0	b413.0	b413.0	b414.0	b412.0	b411.5
9C	70.3	8321	299.8	327.6	112	23	b424.0	b423.0	b419.0	b424.0	b419.0	b423.0	-----	b419.0	b416.5	b419.0	b419.0	b421.5	b430.0	b419.0
14C	70.3	5579	324.8	343.2	116	19	b415.0	b408.0	b407.0	b410.0	b406.0	b408.0	-----	b409.0	b406.5	b408.0	b409.0	b410.0	b413.0	b409.0
16C	70.6	5674	332.1	350.9	116	53	b418.0	b409.0	b409.0	b409.0	b405.0	b408.0	-----	b409.0	b406.5	b408.0	b406.0	b408.0	b413.0	b405.0
18C	70.9	4854	339.3	355.4	116	56	b409.0	b408.0	b406.5	b408.0	b404.0	b408.0	-----	b409.0	b408.0	b408.0	b406.0	b407.0	b409.0	b405.0
21C	70.5	5295	350.9	368.7	115	77	b422.0	b418.0	b416.5	b419.0	b416.0	b419.0	-----	b418.0	b415.0	b415.0	b414.0	b414.0	b409.0	b410.0
Axial distance from start of heating, z, cm							0.61	1.90	3.12	4.48	5.71	6.96	8.25	9.52	10.79	12.06	12.70	13.33	13.97	13.97
3D	104.3	7439	319.3	335.9	119	24/28	b412.0	b416.0	b416.5	b416.5	b418.0	b415.0	b415.0	b413.0	b413.0	b413.0	b414.0	b414.0	b412.0	b406.5
7D	103.6	4917	338.2	349.3	119	21/22	b393.0	b401.5	b403.0	b399.0	b409.0	b409.0	b409.0	b409.0	b410.0	b411.0	b413.0	b413.0	b410.0	b405.0
10D	103.6	4476	349.8	359.8	119	47/49	b394.0	b402.0	b404.0	b408.0	b409.0	b409.0	b409.0	b408.0	b408.0	b409.0	b408.0	b407.0	b403.0	b403.0
12D	27.4	6777	291.5	347.1	445	<7	b447.0	b446.5	b446.0	b448.0	b449.0	b447.0	b448.0	b446.5	b446.5	b447.0	b450.0	b451.0	b455.0	b445.0
16D	28.2	5327	333.2	375.4	446	0/10	b445.0	b444.0	b444.0	b445.0	b445.0	b444.0	b444.0	b443.0	b442.0	b443.0	b444.0	b444.0	b444.0	b440.0
22D	28.0	3908	385.9	415.9	446	10/34	b439.0	b438.0	b436.5	b437.0	b436.5	b436.0	b435.0	b434.0	b434.0	b434.0	b435.0	b436.5	b436.5	b435.0
24D	14.7	3341	291.5	344.3	445	<7	b437.0	b437.0	b436.0	b436.5	b437.0	b435.0	b436.5	b436.0	b435.0	b437.0	b438.0	b439.0	b439.0	b438.0
30D	14.7	3719	344.3	402.1	446	0/12	b439.0	b439.0	b438.0	b439.0	b438.0	b438.0	b438.0	b438.0	b436.0	b436.0	b436.5	b437.0	b436.5	b436.0
31D	14.4	895	295.4	309.3	113	<7	b356.5	b374.0	b383.0	b387.0	b391.5	b392.0	b394.0	b395.0	b396.5	b397.0	b398.0	b398.0	b398.0	b395.0
32D	14.7	3184	295.9	345.9	114	<7	b398.0	b399.0	b401.5	b403.0	b403.0	b402.0	b402.0	b403.0	b402.0	b403.0	b401.5	b404.0	b405.0	b401.0
37D	14.4	3133	295.9	345.9	689	6	b450.0	b450.0	b450.0	b450.0	b450.0	b449.0	b451.0	b451.5	b451.5	b453.0	b454.0	b455.0	b454.0	b452.0
38D	14.7	4823	296.5	372.1	689	8/10	b456.0	b456.5	b457.0	b458.0	b458.0	b457.0	b457.0	b456.5	b456.5	b458.0	b459.0	b459.0	b456.5	b455.0
47D	14.4	3111	389.3	434.3	687	12/17	b453.0	b451.5	b451.5	b451.5	b451.5	b450.0	b450.0	b450.0	b450.0	b450.0	b451.0	b451.0	b448.0	b449.0
48D	28.2	8353	297.1	364.3	687	9/13	b461.5	b465.0	b464.0	b467.0	b467.0	b465.0	b465.0	b465.0	b465.0	b465.0	b465.0	b466.0	b464.0	b460.0
56D	28.2	4381	399.8	433.2	687	31/38	b454.0	b454.0	b453.0	b454.0	b454.0	b453.0	b453.0	b453.0	b453.0	b454.0	b455.0	b455.0	b452.0	b451.0
57D	141.2	11410	306.5	325.9	123	38/55	b419.0	b421.5	b421.5	b425.0	b426.5	b423.0	b424.0	b422.0	b422.0	b422.0	b424.0	b423.0	b421.5	b412.0

<sup>a</sup>Nonboiling.

<sup>b</sup>Subcooled boiling.

<sup>c</sup>Automatic shutdown after data taken.

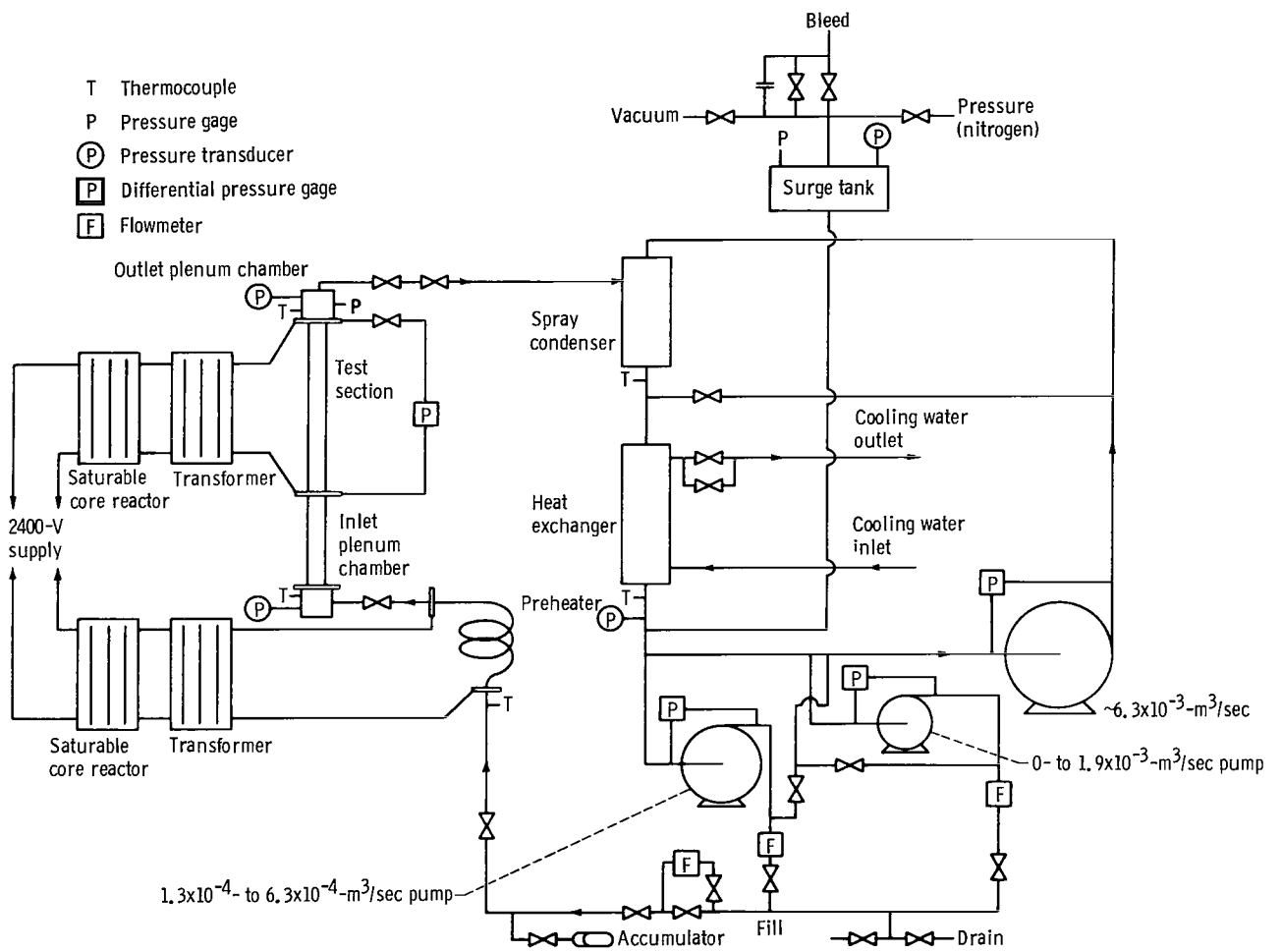


Figure 1. - System flow diagram.

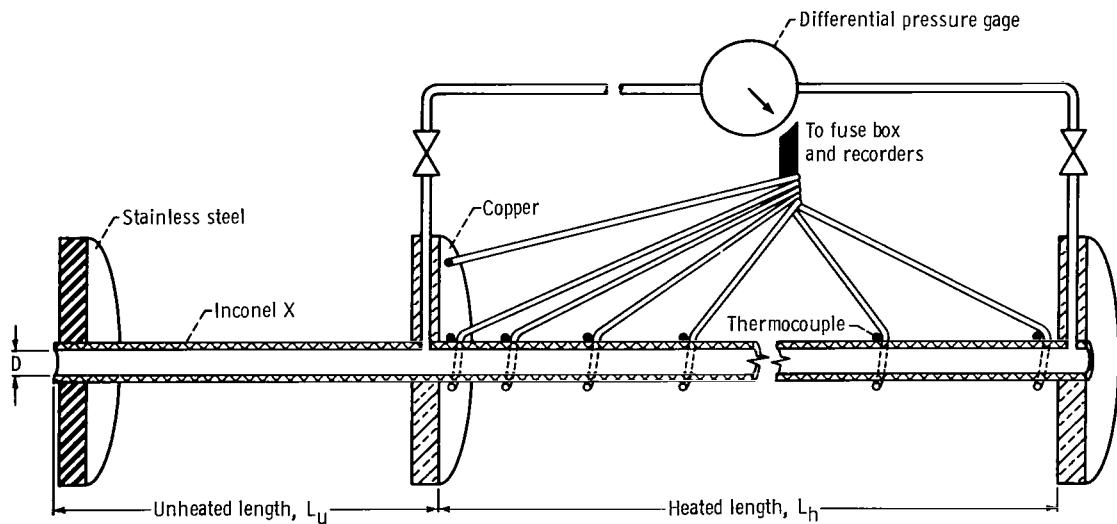


Figure 2. - Schematic diagram of typical test section.

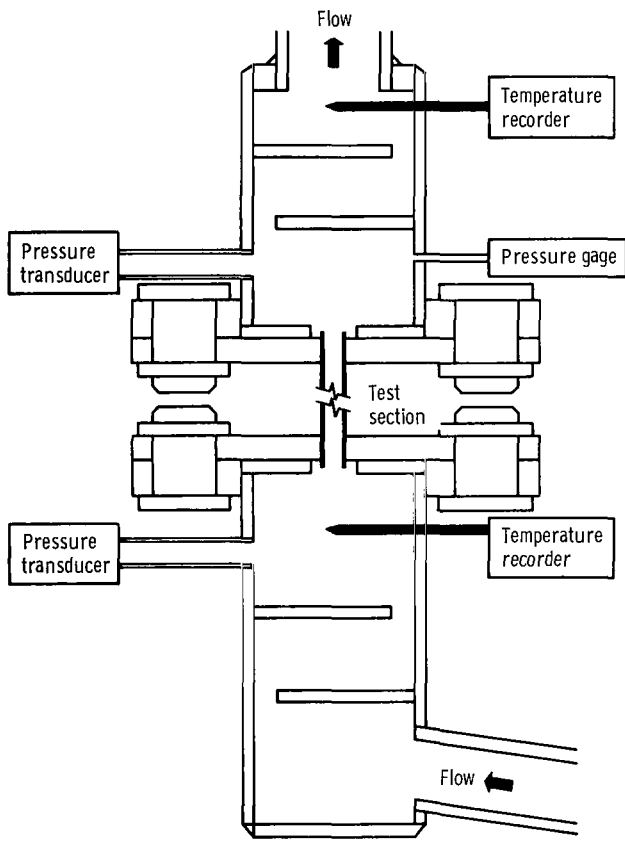


Figure 3. - Plenum chambers.

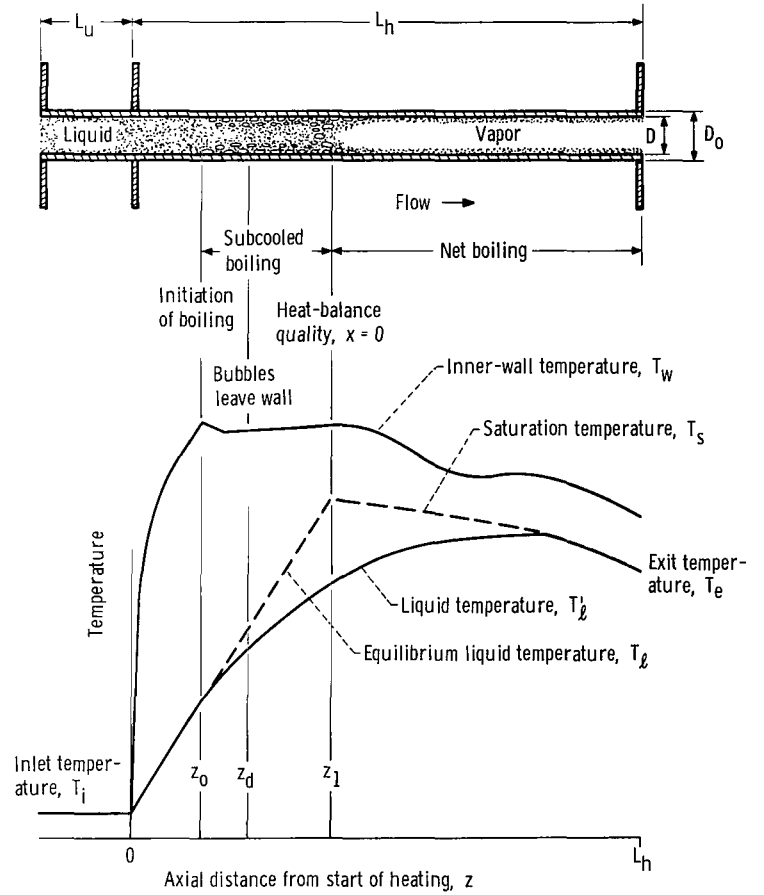


Figure 4. - Typical temperature and voidage profiles with definition of terminology.

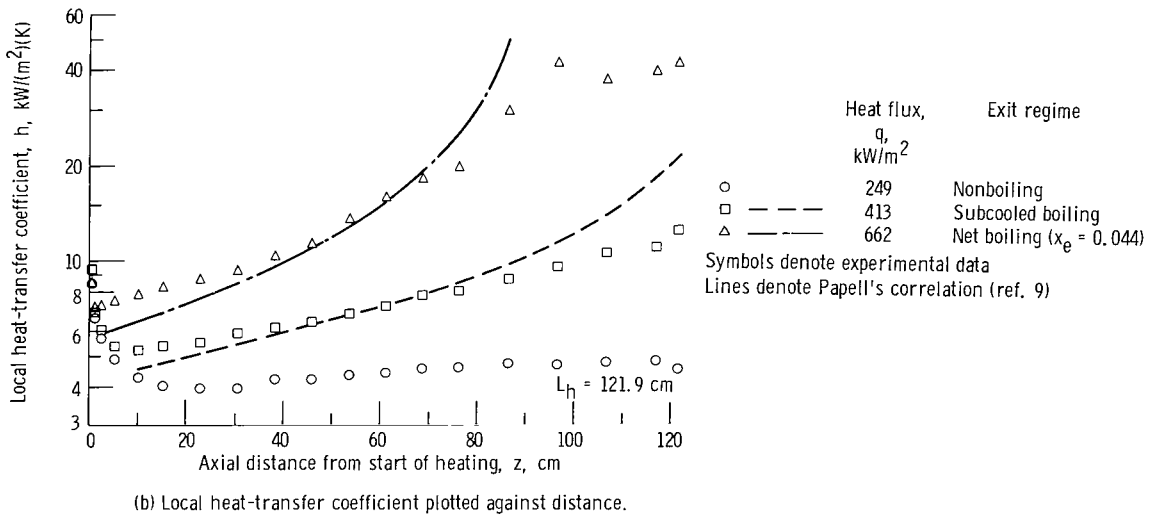
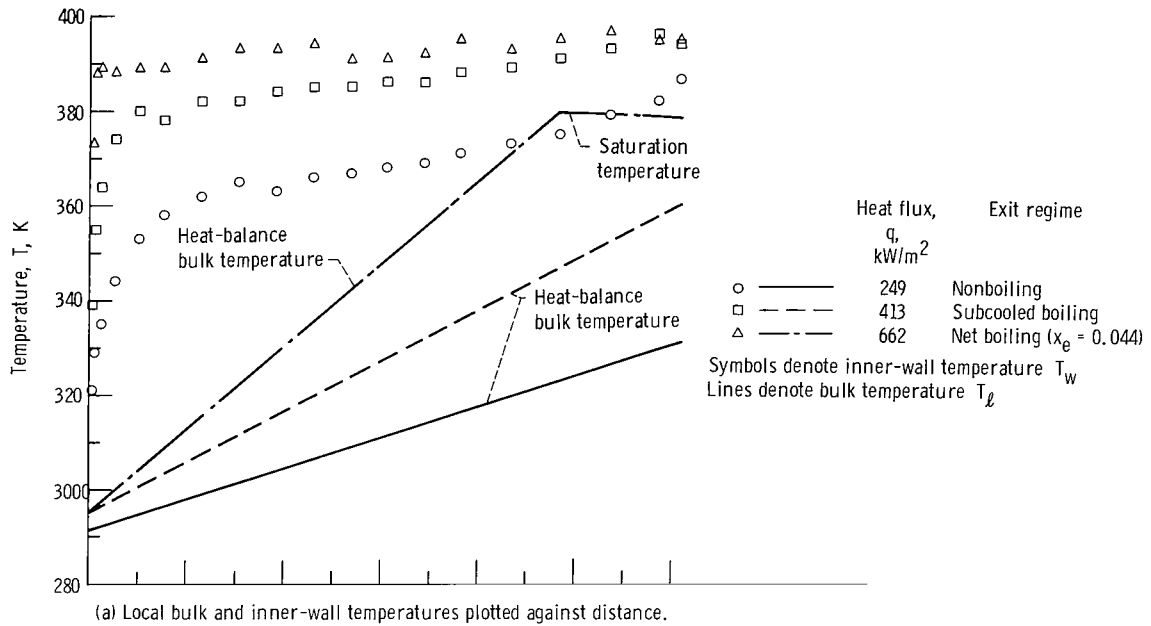
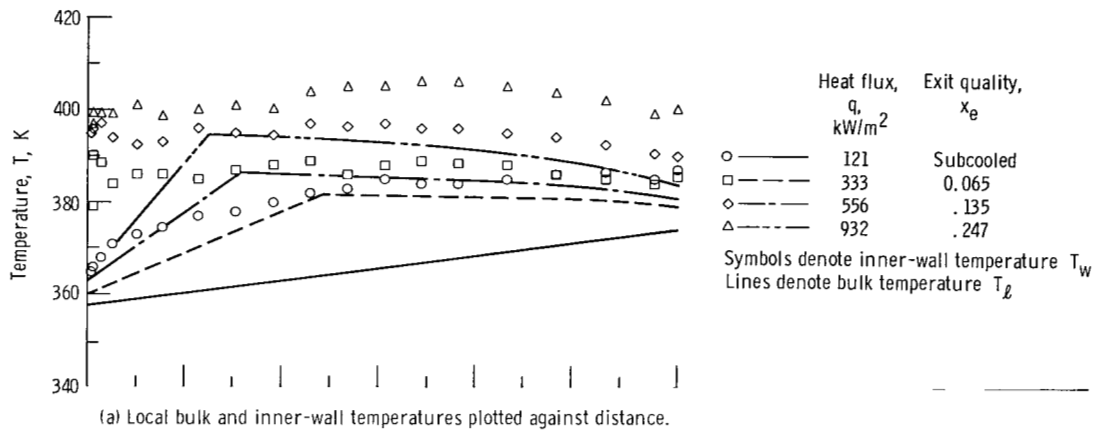
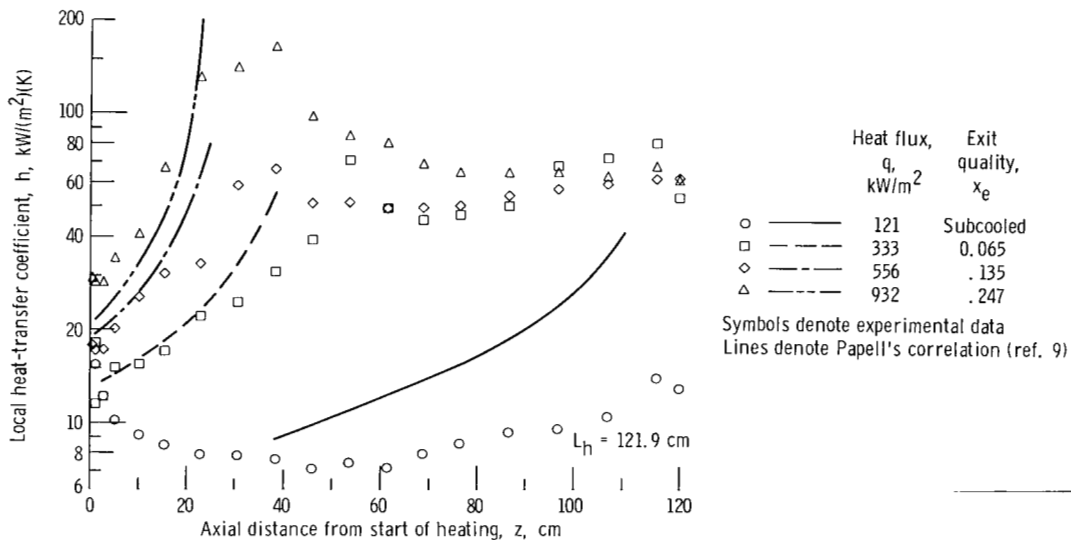


Figure 5. - Typical heat-transfer data for large subcooling at inlet ( $\sim 83 \text{ K}$ ). Tube inside diameter  $D = 1.219 \text{ centimeters}$ ; mass velocity  $G \approx 5.9 \text{ kg}/(\text{sec}/\text{m}^2)$ ; exit pressure  $P_e \approx 117 \text{ kN}/\text{m}^2 \text{ abs}$ .





(a) Local bulk and inner-wall temperatures plotted against distance.



(b) Local heat-transfer coefficients plotted against distance.

Figure 6. - Typical heat-transfer data for small subcooling at inlet (~22 K). Tube inside diameter  $D = 1.219$  centimeters; mass velocity  $G \approx 5.9 \text{ kg/(sec)(m}^2\text{)}$ ; exit pressure  $P_e = 119$  to  $146 \text{ kN/m}^2 \text{ abs}$ .

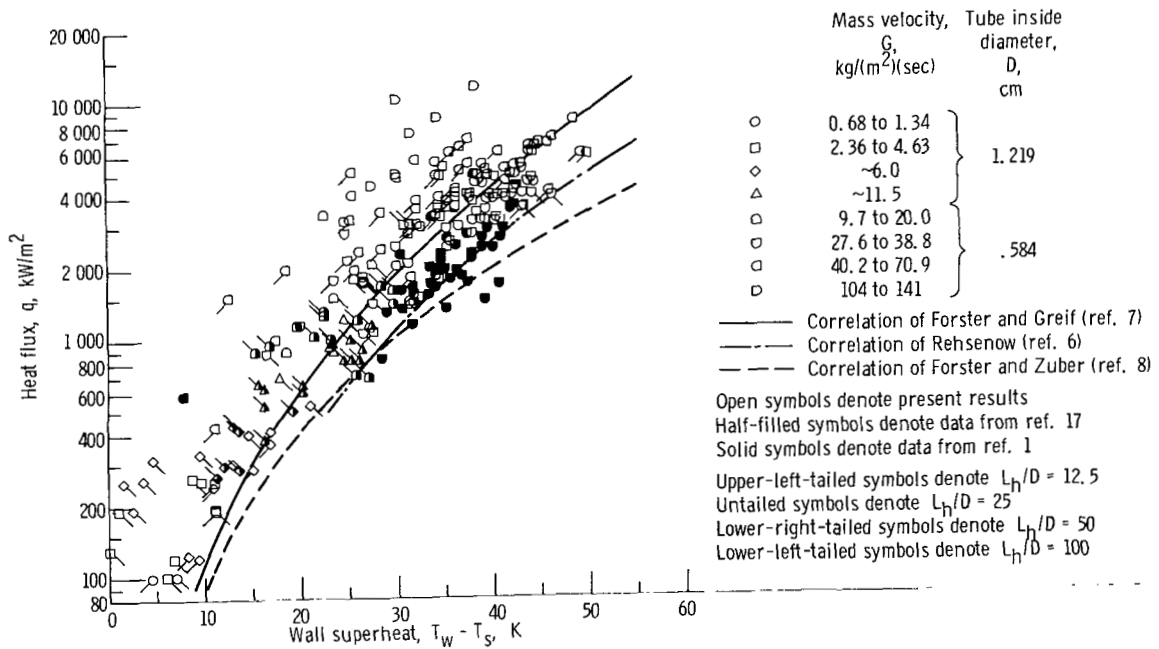


Figure 7. - Heat flux plotted against wall superheat during subcooled boiling for various mass velocities and subcoolings. Exit pressure  $P_e \approx 114 \text{ kN/m}^2 \text{ abs.}$

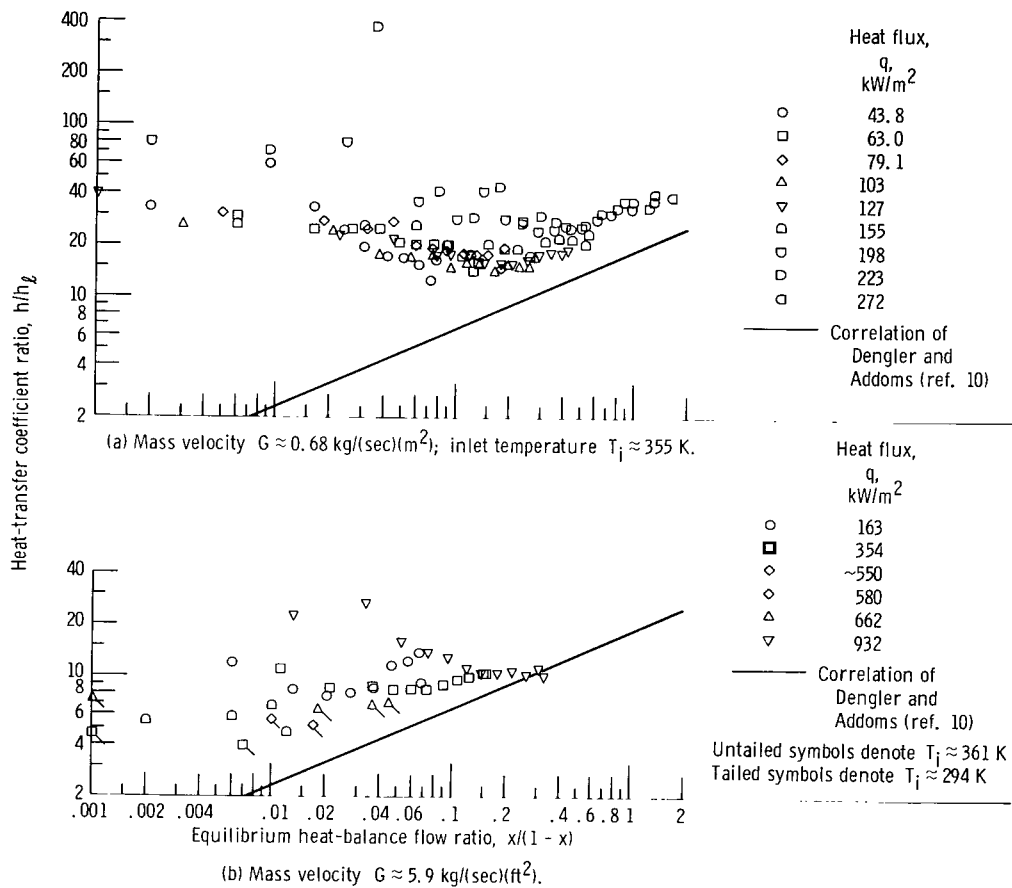


Figure 8. - Ratio of boiling to liquid heat-transfer coefficients plotted against equilibrium heat-balance flow ratio  $x/(1-x)$ . Test section 480-100M (table I); exit pressure  $P_e \approx 117 \text{ kN/m}^2 \text{ abs.}$

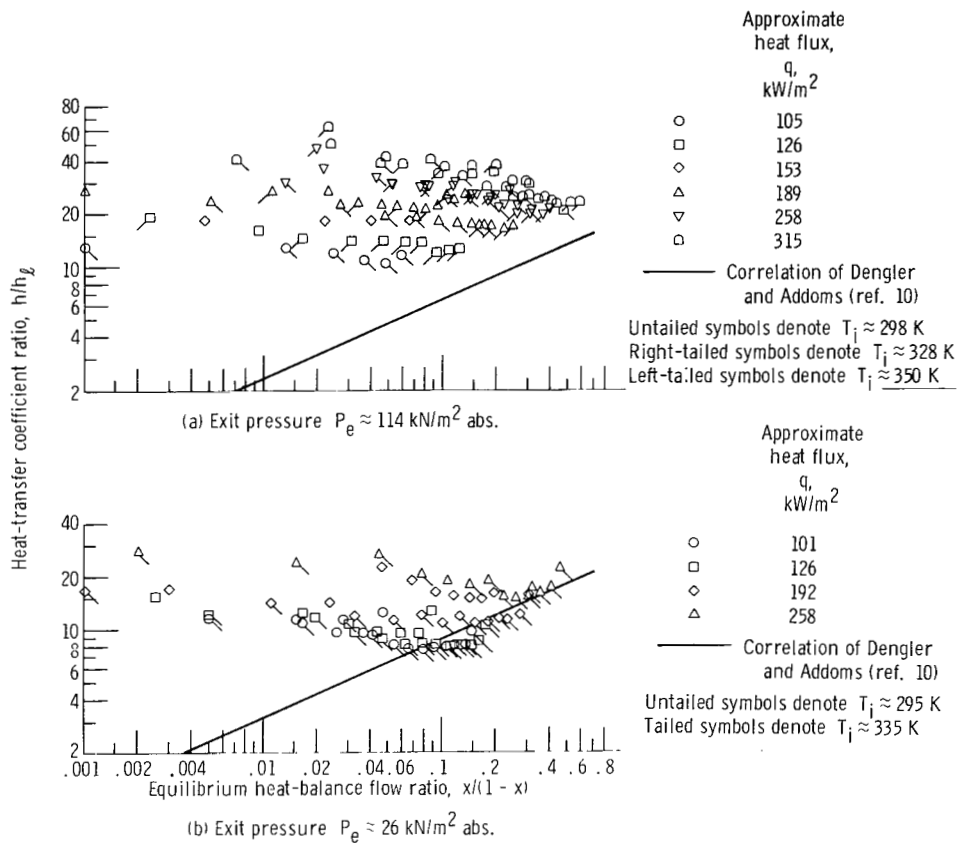
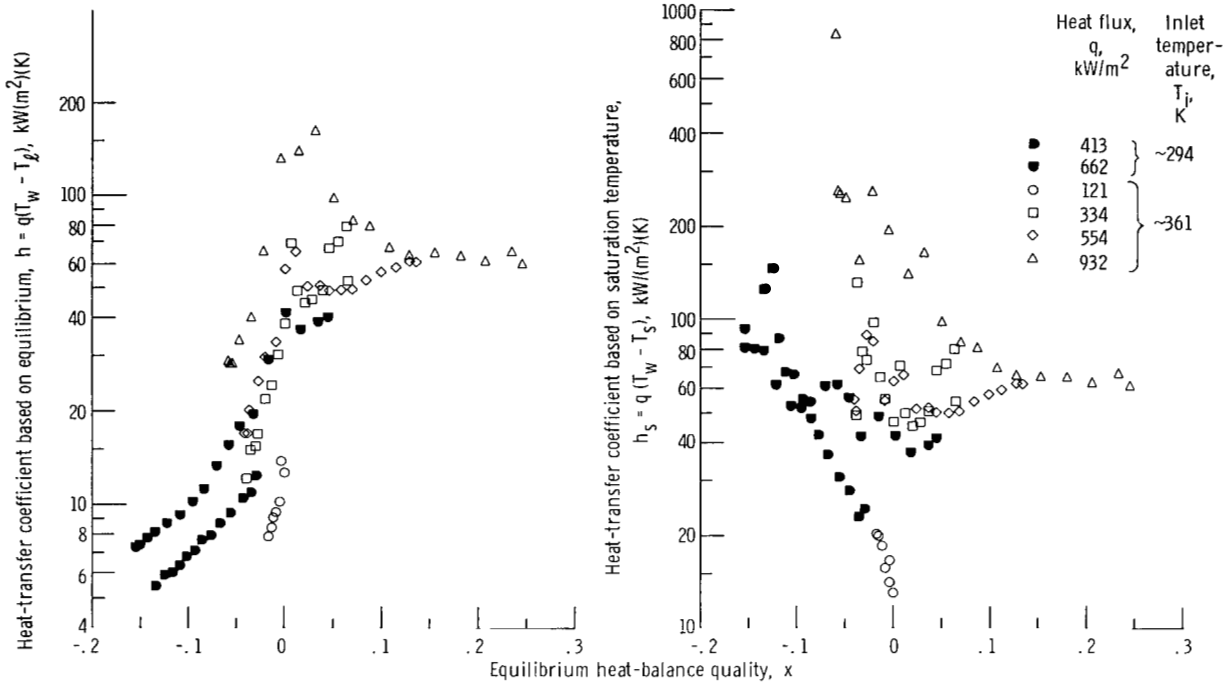
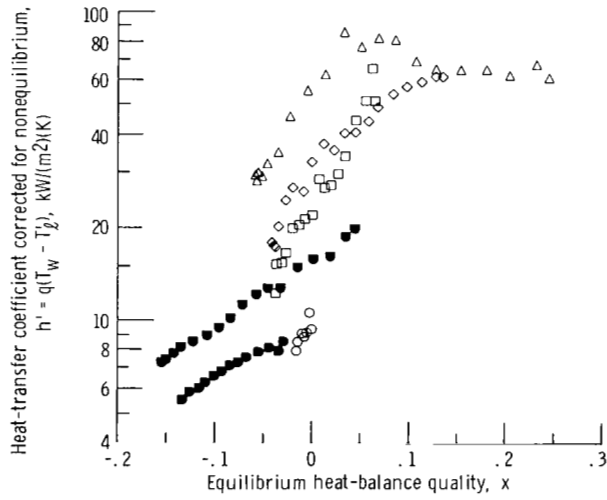


Figure 9. - Ratio of boiling to liquid heat-transfer coefficients plotted against equilibrium heat-balance flow ratio  $x/(1-x)$ . Test section 480-50M (table II); mass velocity  $G \approx 0.68 \text{ kg/(sec)(m}^2\text{)}$ .



(a) Heat-transfer coefficient based on equilibrium heat-balance or saturation temperature.

(b) Heat-transfer coefficient based on saturation temperature.



(c) Heat-transfer coefficient corrected for nonequilibrium.

Figure 10. - Heat-transfer coefficient plotted against equilibrium heat-balance quality for various methods of calculating heat-transfer coefficient. Test section 480-100M (table I); mass velocity  $G \approx 5.9$  kg/(sec)(m<sup>2</sup>); exit pressure  $P_e \approx 119$  to 146 kN/m<sup>2</sup> abs.

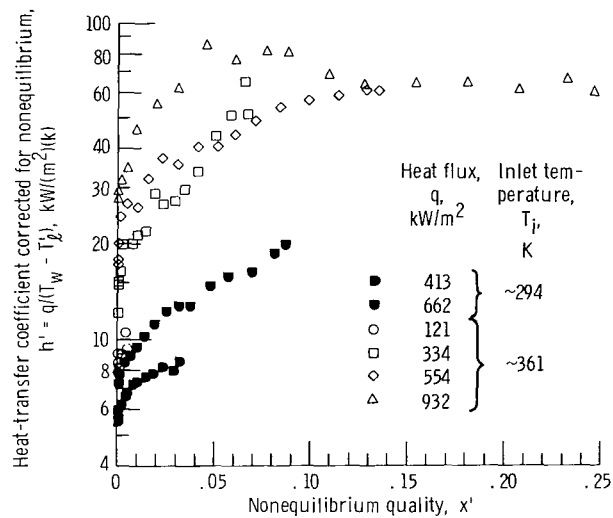


Figure 11. - Heat-transfer coefficient corrected for nonequilibrium plotted against nonequilibrium quality. Test section 480-100M (table I); mass velocity  $G \approx 5.94$  kg/(sec)(m<sup>2</sup>); exit pressure  $P_e \approx 119$  to  $146$  kN/m<sup>2</sup> abs.

NATIONAL AERONAUTICS AND SPACE ADMINISTRATION

WASHINGTON, D. C. 20546

OFFICIAL BUSINESS

PENALTY FOR PRIVATE USE \$300

FIRST CLASS MAIL



POSTAGE AND FEES PAID  
NATIONAL AERONAUTICS AND  
SPACE ADMINISTRATION

003 001 C1 U 33 710701 S00903DS  
DEPT OF THE AIR FORCE  
WEAPONS LABORATORY /WLOL/  
ATTN: E LOU BOWMAN, CHIEF TECH LIBRARY  
KIRTLAND AFB NM 87117

POSTMASTER: If Undeliverable (Section 158  
Postal Manual) Do Not Return

*"The aeronautical and space activities of the United States shall be conducted so as to contribute . . . to the expansion of human knowledge of phenomena in the atmosphere and space. The Administration shall provide for the widest practicable and appropriate dissemination of information concerning its activities and the results thereof."*

— NATIONAL AERONAUTICS AND SPACE ACT OF 1958

## NASA SCIENTIFIC AND TECHNICAL PUBLICATIONS

**TECHNICAL REPORTS:** Scientific and technical information considered important, complete, and a lasting contribution to existing knowledge.

**TECHNICAL NOTES:** Information less broad in scope but nevertheless of importance as a contribution to existing knowledge.

**TECHNICAL MEMORANDUMS:** Information receiving limited distribution because of preliminary data, security classification, or other reasons.

**CONTRACTOR REPORTS:** Scientific and technical information generated under a NASA contract or grant and considered an important contribution to existing knowledge.

**TECHNICAL TRANSLATIONS:** Information published in a foreign language considered to merit NASA distribution in English.

**SPECIAL PUBLICATIONS:** Information derived from or of value to NASA activities. Publications include conference proceedings, monographs, data compilations, handbooks, sourcebooks, and special bibliographies.

**TECHNOLOGY UTILIZATION PUBLICATIONS:** Information on technology used by NASA that may be of particular interest in commercial and other non-aerospace applications. Publications include Tech Briefs, Technology Utilization Reports and Technology Surveys.

*Details on the availability of these publications may be obtained from:*

**SCIENTIFIC AND TECHNICAL INFORMATION OFFICE**

**NATIONAL AERONAUTICS AND SPACE ADMINISTRATION**

**Washington, D.C. 20546**